Journal of Solid Mechanics Vol. 12, No. 4 (2020) pp. 912-934
DOI: 10.22034/jsm.2020.1897751.1579

Analysis of Reflection Phenomena in a Fiber Reinforced Piezo-Thermoelastic Half Space with Diffusion and Two-Temperature

K. Jain [1,*], S. Kumar [2], S. Deswal [1]

[1]*Department of Mathematics, Guru Jambheshwar University of Science and Technology, Hisar-125001, Haryana, India*
[2]*Department of Basic and Applied Sciences, BPS Mahila Vishwavidyalaya, Khanpur Kalan, Sonepat-131305, Haryana, India*

Received 3 August 2020; accepted 5 October 2020

ABSTRACT

Present work is concerned with the analysis of transient wave phenomena in a piezo-thermoelastic medium with diffusion, fiber reinforcement and two-temperature, when an elastic wave is made incident obliquely at the traction free plane boundary of the considered medium. The formulation is applied under the purview of generalized theory of thermoelasticity with one relaxation time. The problem is solved analytically and it is found that there exists four coupled quasi waves: *qP* (quasi-*P*), *qMD* (quasi mass diffusion), *qT* (quasi thermal) and *qSV* (quasi-*SV*) waves propagating with different speeds in a two-dimensional model of the solid. The amplitude ratios, phase velocities and energy ratios for the reflected waves are derived and the numerical computations have been carried out with the help of MATLAB programming. Effect of presence of diffusion is analyzed theoretically, numerically and graphically. The number of reflected waves reduce to three in the absence of diffusion as *qMD* wave will disappear in that case which is physically admissible. Influence of piezoelectric effect, two temperature and anisotropy is discussed on different characteristics of reflected waves such as phase velocity and reflection coefficients. It has been verified that there is no dissipation of energy at the boundary surface during reflection. Thus, the energy conservation law holds at the surface. Finally, all the reflection coefficients are represented graphically through 3D plots to estimate and highlight the effects of frequency and angle of incidence.

Keywords: Generalized thermoelasticity; Piezo-thermoelasticity; Fiber reinforcement; Two-temperature; Diffusion; Reflection phenomena.

1 INTRODUCTION

In solid mechanics, the medium is regarded as continuous and one of the most important branches of continuum mechanics is the classical theory of elasticity which is concerned with the systematic study of the response of elastic bodies to the action of forces which deform it. After that, the theory of elasticity was extended to include

*Corresponding author. Tel.: +91 8059751400.
E-mail address: kavitaj217@gmail.com (K. Jain).

thermal effects. This new theory was called 'Thermoelasticity'. Biot [1] developed the coupled theory of thermoelasticity to overcome the paradox inherent in the uncoupled theory that elastic changes have no effect on temperature. But the parabolic type of heat conduction equation, as was used initially in the study of thermoelastic behaviour was found to yield some unrealistic situation in the sense that the velocity of heat signals was infinite. Generalized thermoelastic theories have been developed with the objective of removing this defect of coupled theory. The extended thermoelasticity theory introducing one relaxation time in the thermoelastic process was proposed by Lord and Shulman [2] who obtained a wave-type heat equation by predicating a new law of heat conduction. This new law contains the heat flux vector as well as its time derivative and a new constant in Fourier's law of heat conduction. The introduced new constant acts as a relaxation time *i.e.* the time lag needed to establish steady state heat flow in the medium. Ignaczak and Ostoja-Starzewski [3] focused on the mathematical aspects of the generalized thermoelasticity theories. Several notable works regarding the study of the phenomena of wave propagation for the better elucidation of the thermal properties of different media under the purview of different theories of generalized thermoelasticity with various conditions have been performed by Lata [4,5] and Lata and Kaur [6]. Recently, Lata and Kaur [7] investigated behaviour of different field variables in two dimensional transversely isotropic magneto thermoelastic solid with rotation due to time-harmonic source. The problem was formulated using generalized thermoelasticity theory with one relaxation time and solved with the help of Fourier transformation technique. Piezoelectric materials are commonly used for smart structure applications due to their direct and converse piezoelectric effects, which allow them to be utilized as both actuators and sensors. The internal generation of an electrical charge from an applied mechanical force is known as direct piezoelectric effect. The internal generation of a mechanical strain resulting from an applied electric field is known as converse piezoelectric effect. The piezo-thermoelastic material response entails an interaction of three major fields, namely, mechanical, thermoelastic and electric field in the macro-physical world. The thermo-piezoelectric material has one important application to detect the responses of a structure by measurement of the electric charge, sensing or to reduce excessive responses by applying additional electric forces or thermal forces. Among the early investigations in this area, Mindlin [8] studied the electromechanical couplings of linear piezo-thermoelastic medium. Nowacki [9-11] investigated the physical laws for the thermo-piezoelectric materials. Thereafter, Chandrasekharaiah [12,13] used generalized Mindlin's theory in order to study the finite speed of propagation of thermal disturbances. The wave propagation problems in piezoelectric media are also used in applications, such as aerospace engineering, mechanical engineering, civil engineering and bio-engineering. Reflection and transmission of acoustic energy at boundary surface plays an important role in the areas like signal processing, transduction and frequency control. A number of problems, which are related to the phenomena of reflection and refraction of plane waves for piezoelectric materials, can be found in the literature (Sharma et al. [14], Kuang and Yuan [15], Yuan and Jiang [16]). The reflection and transmission of plane waves from a fluid-piezothermoelastic solid interface was studied by Vashishth and Sukhija [17]. Othman and Ahmed [18] applied three different thermoelastic theories namely, coupled theory, Lord-Shulman theory and Green-Lindsay with two relaxation times, to study the deformation of a generalized piezo-thermoelastic rotating medium under the influence of gravity and magnetic field. A reinforced concrete member is designed for all conditions of stress that may occur in accordance with the principle of mechanics. Fiber reinforced composites are bound together as a single unit so that there can be no relative displacement between them *i.e.* they act together as a single anisotropic unit. The artificial structures on the surface of the earth are excited during an earthquake, which give rise to violent vibrations in some cases. Engineers and architects are in search of such reinforced elastic materials for the structures that resist the oscillatory vibrations. Pipkin [19] and Rogers [20] did inspiring work in this field. The idea of continuous self-reinforcement at every point of an elastic solid was introduced by Belfield et al. [21]. A lot of research work has been done in fiber reinforced thermoelastic medium, during last few years. Notable among them are Singh and Tomar [22] and Abbas et al. [23] and Said and Othman [24]. Analysis of transient wave phenomena in a fiber reinforced generalized rotating thermoelastic medium with two temperature was discussed by Deswal et al. [25]. Recently, Lata and Kaur [26] investigated thermomechanical interactions in homogeneous transversely isotropic magneto thermoelastic medium with fractional order heat transfer and hall current, whose bounding surface is subjected to normal force with weak, normal and strong conductivity.The theory of heat conduction of a deformable body, formulated by Chen and Gurtin [27] and Chen et al. [28,29] depends on two different temperatures: the conductive temperature ϕ and the thermodynamic temperature θ. During the past few decades, it is realized that the models of two-temperature thermoelasticity may be of more relevance to real situations, as it is more logical to assume a second law in which the entropy contribution due to heat conduction is governed by one temperature, that of the heat supply by another. Youssef [30] developed a new theory of two-temperature generalized thermoelasticity by using the theory of heat conduction in deformable bodies and obtained the uniqueness theorem. Some one dimensional problems in generalized two-temperature piezo-thermoelastic medium have been solved by Youssef and Bassiouny [31] and

Islam and Kanoria [32]. Kaur and Lata [33] studied the plane wave propagation with combined effect of hall current and two temperature in generalized magneto thermoelastic medium. Freshly, Lata and Kaur [34] depicted the thermomechanical interactions in transversely isotropic magneto thermoelastic solid with two temperatures and without energy dissipation. The effect of two temperature and relaxation time are presented graphically on the resulting quantities. Thermodiffusion in elastic solids is due to the coupling of fields of temperature, mass diffusion and that of strain, in addition to heat and mass exchange with the environment. Nowacki [35-37] developed the theory of thermoelastic diffusion and studied dynamical problems of diffusion in solids. Sherief et al. [38] developed the theory of generalized thermoelastic diffusion that predicts finite speeds of propagation for thermoelastic and diffusive waves. Kuang [39] discussed the variational principles for generalized thermodiffusion theory in pyroelectricity. Kumar and Chawla [40] obtained the general steady-state solution and Green's function for an orthotropic piezothermoelastic diffusive medium. The propagation of harmonic plane waves in a homogeneous anisotropic piezo-thermoelastic diffusive medium was discussed by Kumar and Sharma [41]. Kaur and Lata [42] investigated Rayleigh wave propagation in a transversely isotropic magneto-thermoelastic medium with fractional order three-phase-lag heat transfer. In recent times, Kansal [43] proposed the fundamental solution of partial differential equations in the generalized theory of thermoelastic diffusion materials with double porosity.

The study of reflection and refraction phenomena in piezoelectric materials has gained considerable attention due to their important role in hydrophone technology, aerospace engineering, civil engineering and in general ultrasonic transducer application. Till now, no analysis has been done on wave propagation in a fiber reinforced piezo-thermoelastic medium with diffusion and two-temperature. Hence, to address this issue, we have solved a two-dimensional problem in such type of medium. The generalized theory of thermoelasticity with one relaxation time has been employed for addressing the mathematical analysis. The efforts of this research are focused on systematically studying the various characteristics of reflected waves in the medium when a set of coupled waves strikes obliquely at boundary surface of the assumed model and their variations with angle of incidence are presented graphically. Further the effects of considered parameters are analyzed in generalized thermoelastic medium. Finally, we present a discussion of the results and make some concluding remarks. The results are validated by comparing them with those cited in literature as special cases.

2 NOMENCLATURE

$\mathbf{u}$	dynamic displacement vector, m
σ_{ij}	components of stress tensor, $kgm^{-1}s^{-2}$
e_{ij}	components of strain tensor,
e_{kk}	dilatation,
δ_{ij}	Kronecker delta,
λ, μ_T	elastic constants, $kgm^{-1}s^{-2}$
$\alpha, \beta, (\mu_L - \mu_T)$	fiber reinforcement parameters, $kgm^{-1}s^{-2}$
ρ	density of the medium, kgm^{-3}
c_E	specific heat at constant strain, $Jkg^{-1}K^{-1}$
K_{ij}	thermal conductivity tensor, $Jm^{-1}K^{-1}s^{-1}$
ϕ	conductive temperature, K
$\theta = T - T_0$	thermodynamical temperature, K
T	absolute temperature, K
T_0	temperature of the medium in its natural state assumed to be $\left\|\frac{\theta}{T_0}\right\| << 1$, K
a_{ij}	two-temperature parameters, m^2
$c = C - C_0$,	
C	non-equilibrium concentration, kgm^{-3}

C_0 mass concentration at natural state, kgm^{-3}

β_{ij} thermoelastic coupling tensor, $kgm^{-1}s^{-2}K^{-1}$

γ_{ij} thermodiffusive coupling tensor, m^2s^{-2}

α_{ij} coefficients of linear thermal expansion, K^{-1}

v_{ij} coefficients of linear diffusion expansion, m^3kg^{-1}

a measure of thermodiffusion effect, $m^2s^{-2}K^{-1}$

b measure of diffusion effect, $m^5kg^{-1}s^{-2}$

D_{ij} thermodiffusion tensor, $kgsm^{-3}$

τ_0 thermal relaxation time, s

τ_0 dffusion relaxation time, s

D electric displacement vector, Cm^{-2}

E electric field intensity vector, $kgms^{-2}C^{-1}$

ψ electric potential, $kgm^2s^{-2}C^{-1}$

b_i piezoelectric coefficients, $kg^{-1}Cm$

$\in_{ij}$ dielectric permittivity coefficients, $kg^{-1}m^{-3}s^2$

p_i pyroelectric coefficients, $CK^{-1}m^{-2}$

η_{ijk} piezoelectric constants, Cm^{-2}

ψ_0 electric potential in the natural state, $kgm^2s^{-2}C^{-1}$

3 GOVERNING EQUATIONS

Following Vashishth and Sukhija [17], Belfield et al. [21] and Kumar and Sharma [41], the constitutive equations and the field equations for a homogeneous, transversely isotropic, fiber reinforced piezo-thermoelastic half space with diffusion and two-temperature in the context of Lord and Shulman model, are given as follows:

(i) Constitutive relations

$$\sigma_{ij} = \lambda e_{kk}\delta_{ij} + 2\mu_T e_{ij} + \alpha\left(a_k a_m e_{km}\delta_{ij} + a_i a_j e_{kk}\right) + 2\left(\mu_L - \mu_T\right)\left(a_i a_k e_{kj} + a_j a_k e_{ki}\right) + \beta a_k a_m e_{km} a_i a_j - \beta_{ij}\theta - \gamma_{ij}c - \eta_{kij}E_k, \tag{1}$$

where $e_{ij} = \dfrac{u_{i,j} + u_{j,i}}{2}$ and $\vec{a} = (a_1, a_2, a_3), a_1^2 + a_2^2 + a_3^2 = 1$.

(ii) Equation of motion

$$\sigma_{ji,j} = \rho\ddot{u}_i, \tag{2}$$

(iii) Equation of heat conduction

$$K_{ij}\phi_{,ij} = \left(1 + \tau_0\frac{\partial}{\partial t}\right)\left(\rho c_E\dot{\theta} + T_0\left(\beta_{ij}\dot{u}_{i,j} - p_k\dot{\psi}_{,k} + a\dot{c}\right)\right), \tag{3}$$

(iv) Equation of mass diffusion

$$D_{ij}bc_{,ij} = D_{ij}\left(\gamma_{ij}u_{i,jij} + a\theta_{,ij} + b_i\psi_{,iij}\right) + \left(1 + \tau^0\frac{\partial}{\partial t}\right)\dot{c}, \tag{4}$$

(v) Gauss equation

$$\begin{aligned} &D_{i,i} = 0, \\ &D_i = \eta_{ijk} e_{jk} + \in_{ij} E_j + p_i \theta + b_i c, \end{aligned} \tag{5}$$

where $E_i = -\psi_{,i}$.

(vi) Relation between thermodynamical and conductive temperature

$$\phi - \theta = a_{ij} \phi_{,ij}. \tag{6}$$

Comma notation denotes partial derivatives with respect to spatial co-ordinates and dot notation represents derivative with respect to time.

The thermal conductivity tensor, thermal and diffusion elastic coupling tensor and thermodiffusion tensor satisfy the following symmetric relations:

i. $K_{ij} = K_i \delta_{ij} (K_{ij} = K_{ji})$,

ii. $\beta_{ij} = \beta_i \delta_{ij} (\beta_{ij} = \beta_{ji})$,

iii. $\gamma_{ij} = \gamma_i \delta_{ij} (\gamma_{ij} = \gamma_{ji})$,

iv. $D_{ij} = D_i^{'} \delta_{ij} (D_{ij} = D_{ji})$ respectively and i is not summed.

4 FORMULATION OF THE PROBLEM

We consider the problem of a fiber-reinforced piezo-thermoelastic diffusive half space with two-temperature in the context of Lord and Shulman theory. The rectangular cartesian co-ordinates are introduced having origin on the surface $z = 0$ and z-axis pointing vertically downwards into the medium, so that the half space occupies the region $z \geq 0$. We choose the fiber reinforcement direction as $\vec{a} = (0, 0, 1)$ *i.e.* along z-axis. The poling axis of the piezoelectric material is also assumed to coincide with z-axis. The traction free surface $z = 0$ is subjected to isothermal boundary conditions. Our analysis is restricted to a two dimensional problem in xz-plane so that all the considered functions will depend on time t and the co-ordinates x and z.

Thus $\mathbf{u} = (u, 0, w)$, $\mathbf{E} = (E_1, 0, E_3)$ and $\frac{\partial}{\partial y} = 0$, so that the constitutive relations and field equations reduce to the following form:

$$\sigma_{zz} = A_{11} \frac{\partial u}{\partial x} + A_{12} \frac{\partial w}{\partial z} + \eta_{33} \frac{\partial \psi}{\partial z} - \beta_3 \theta - \gamma_3 c, \tag{7}$$

$$\sigma_{zx} = \sigma_{xz} = A_{13} \left(\frac{\partial u}{\partial z} + \frac{\partial w}{\partial x} \right) + \eta_{15} \frac{\partial \psi}{\partial x}, \tag{8}$$

$$\sigma_{xx} = A_{14} \frac{\partial u}{\partial x} + A_{11} \frac{\partial w}{\partial z} + \eta_{31} \frac{\partial \psi}{\partial z} - \beta_1 \theta - \gamma_1 c, \tag{9}$$

$$A_{14} \frac{\partial^2 u}{\partial x^2} + A_{15} \frac{\partial^2 w}{\partial x \partial z} + A_{13} \frac{\partial^2 u}{\partial z^2} + A_{16} \frac{\partial^2 \psi}{\partial x \partial z} - \beta_1 \frac{\partial \theta}{\partial x} - \gamma_1 \frac{\partial c}{\partial x} = \rho \frac{\partial^2 u}{\partial t^2}, \tag{10}$$

$$A_{13} \frac{\partial^2 w}{\partial x^2} + A_{15} \frac{\partial^2 u}{\partial x \partial z} + A_{12} \frac{\partial^2 w}{\partial z^2} + \eta_{33} \frac{\partial^2 \psi}{\partial z^2} + \eta_{15} \frac{\partial^2 \psi}{\partial x^2} - \beta_3 \frac{\partial \theta}{\partial z} - \gamma_3 \frac{\partial c}{\partial z} = \rho \frac{\partial^2 w}{\partial t^2}, \tag{11}$$

$$K_1\frac{\partial^2\phi}{\partial x^2}+K_3\frac{\partial^2\phi}{\partial z^2}=\frac{\partial}{\partial t}\left(1+\tau_0\frac{\partial}{\partial t}\right)\left(\rho c_E\theta+T_0\left(\beta_1\frac{\partial u}{\partial x}+\beta_3\frac{\partial w}{\partial z}+ac-p_3\frac{\partial\psi}{\partial z}\right)\right), \tag{12}$$

$$\begin{aligned}&D_1'\left(\gamma_1\frac{\partial^3 u}{\partial x^3}+\gamma_3\frac{\partial^3 w}{\partial x^2\partial z}+a\frac{\partial^2\theta}{\partial x^2}+b_3\frac{\partial^3\psi}{\partial x^2\partial z}\right)+D_3'\left(\gamma_1\frac{\partial^3 u}{\partial z^2\partial x}+\gamma_3\frac{\partial^3 w}{\partial z^3}+a\frac{\partial^2\theta}{\partial z^2}+b_3\frac{\partial^3\psi}{\partial z^3}\right)\\&+\frac{\partial}{\partial t}\left(1+\tau^0\frac{\partial}{\partial t}\right)c=b\left(D_1'\frac{\partial^2 c}{\partial x^2}+D_3'\frac{\partial^2 c}{\partial z^2}\right),\end{aligned} \tag{13}$$

$$D_1=\eta_{15}\left(\frac{\partial u}{\partial z}+\frac{\partial w}{\partial x}\right)-\in_{11}\frac{\partial\psi}{\partial x}, \tag{14}$$

$$D_3=\eta_{31}\frac{\partial u}{\partial x}+\eta_{33}\frac{\partial w}{\partial z}-\in_{33}\frac{\partial\psi}{\partial z}+p_3\theta+b_3 c, \tag{15}$$

$$\eta_{15}\frac{\partial^2 w}{\partial x^2}+\eta_{33}\frac{\partial^2 w}{\partial z^2}+A_{16}\frac{\partial^2 u}{\partial x\,\partial z}-\in_{11}\frac{\partial^2\psi}{\partial x^2}-\in_{33}\frac{\partial^2\psi}{\partial z^2}+p_3\frac{\partial\theta}{\partial z}+b_3\frac{\partial c}{\partial z}=0, \tag{16}$$

$$\phi-\theta=a_{11}\frac{\partial^2\phi}{\partial x^2}+a_{33}\frac{\partial^2\phi}{\partial z^2}, \tag{17}$$

where

$$\begin{aligned}&\beta_1=(2\lambda+\alpha)\alpha_{33}+(\lambda+2\mu_T)\alpha_{11},\\&\beta_3=(2\lambda+3\alpha+4\mu_L-2\mu_T+\beta)\alpha_{33}+(\lambda+\alpha)\alpha_{11},\\&\gamma_1=(2\lambda+\alpha)v_{33}+(\lambda+2\mu_T)v_{11},\\&\gamma_3=(2\lambda+3\alpha+4\mu_L-2\mu_T+\beta)v_{33}+(\lambda+\alpha)v_{11},\\&A_{11}=\lambda+\alpha, A_{12}=\lambda+2\alpha+4\mu_L-2\mu_T+\beta, A_{13}=\mu_L, A_{14}=\lambda+2\mu_T, A_{15}=A_{11}+A_{13}, A_{16}=\eta_{31}+\eta_{15},\end{aligned}$$

To make the field equations simplified, we introduce the following dimensionless transformations

$$\begin{aligned}&(x',z',u',w')=c_1\chi(x,z,u,w),\left(t',\tau_0',\tau^{0'}\right)=c_1^2\chi\left(t,\tau_0,\tau^0\right),\\&(\phi',\theta')=\frac{1}{T_0}(\phi,\theta),c'=\frac{1}{C_0}c,\psi'=\frac{1}{\psi_0}\psi,D'=\frac{\eta_{33}}{\rho c_1^2}D,\\&\sigma_{ij}'=\frac{1}{\rho c_1^2}\sigma_{ij},\left(a_{11}',a_{33}'\right)=c_1^2\chi^2\left(a_{11},a_{33}\right),\end{aligned}$$

where $\chi=\dfrac{\rho c_E}{K_1}$ and $c_1^2=\dfrac{A_{12}}{\rho}$.

In terms of the above non-dimensional quantities, the governing Eqs. (7)-(17) in *xz*-plane reduce to (dropping the dashes for convenience)

$$\sigma_{zz}=\frac{\partial w}{\partial z}+B_{11}\frac{\partial u}{\partial x}+B_{12}\frac{\partial\psi}{\partial z}-B_{13}\theta-B_{14}c, \tag{18}$$

$$\sigma_{zx}=B_{15}\left(\frac{\partial u}{\partial z}+\frac{\partial w}{\partial x}\right)+B_{16}\frac{\partial\psi}{\partial x}, \tag{19}$$

$$\sigma_{xx} = B_{17}\frac{\partial u}{\partial x} + B_{11}\frac{\partial w}{\partial z} + B_{18}\frac{\partial \psi}{\partial z} - B_{19}\theta - B_{10}c, \tag{20}$$

$$B_{17}\frac{\partial^2 u}{\partial x^2} + B_{20}\frac{\partial^2 w}{\partial x\,\partial z} + B_{15}\frac{\partial^2 u}{\partial z^2} + B_{21}\frac{\partial^2 \psi}{\partial x\,\partial z} - B_{19}\frac{\partial \theta}{\partial x} - B_{10}\frac{\partial c}{\partial x} = \frac{\partial^2 u}{\partial t^2}, \tag{21}$$

$$B_{15}\frac{\partial^2 w}{\partial x^2} + B_{20}\frac{\partial^2 u}{\partial x\,\partial z} + \frac{\partial^2 w}{\partial z^2} + B_{16}\frac{\partial^2 \psi}{\partial x^2} + B_{12}\frac{\partial^2 \psi}{\partial z^2} - B_{13}\frac{\partial \theta}{\partial z} - B_{14}\frac{\partial c}{\partial z} = \frac{\partial^2 w}{\partial t^2}, \tag{22}$$

$$\frac{\partial^2 \phi}{\partial x^2} + \varepsilon_1\frac{\partial^2 \phi}{\partial z^2} = \frac{\partial}{\partial t}\left(1 + \tau_0\frac{\partial}{\partial t}\right)\left(\theta + \varepsilon_2\frac{\partial u}{\partial x} + \varepsilon_3\frac{\partial w}{\partial z} + \varepsilon_4 c - \varepsilon_5\frac{\partial \psi}{\partial z}\right), \tag{23}$$

$$\begin{aligned}&\varepsilon_7\frac{\partial^3 u}{\partial x^3} + \varepsilon_8\frac{\partial^3 w}{\partial x^2\partial z} + \varepsilon_9\frac{\partial^2 \theta}{\partial x^2} + \varepsilon_{10}\frac{\partial^3 \psi}{\partial x^2\partial z} + \varepsilon_{11}\frac{\partial^3 u}{\partial z^2\partial x} + \varepsilon_{12}\frac{\partial^3 w}{\partial z^3} + \varepsilon_{13}\frac{\partial^2 \theta}{\partial z^2} + \varepsilon_{14}\frac{\partial^3 \psi}{\partial z^3}\\ &+\varepsilon_{15}\left(1 + \tau^0\frac{\partial}{\partial t}\right)\frac{\partial c}{\partial t} = \frac{\partial^2 c}{\partial x^2} + \varepsilon_6\frac{\partial^2 c}{\partial z^2},\end{aligned} \tag{24}$$

$$D_1 = d_1\left(\frac{\partial u}{\partial z} + \frac{\partial w}{\partial x}\right) - d_2\frac{\partial \psi}{\partial x}, \tag{25}$$

$$D_3 = d_3\frac{\partial u}{\partial x} + d_4\frac{\partial w}{\partial z} - d_5\frac{\partial \psi}{\partial z} + d_6\theta + d_7 c, \tag{26}$$

$$h_1\frac{\partial^2 w}{\partial x^2} + h_2\frac{\partial^2 w}{\partial z^2} + h_3\frac{\partial^2 u}{\partial x\,\partial z} - h_4\frac{\partial^2 \psi}{\partial x^2} - h_5\frac{\partial^2 \psi}{\partial z^2} + h_6\frac{\partial \theta}{\partial z} + h_7\frac{\partial c}{\partial z} = 0, \tag{27}$$

$$\phi - \theta = a_{11}\frac{\partial^2 \phi}{\partial x^2} + a_{33}\frac{\partial^2 \phi}{\partial z^2}. \tag{28}$$

where

$$B_{11} = \frac{A_{11}}{A_{12}}, B_{12} = \frac{\eta_{33}\psi_0 c_1\chi}{A_{12}}, B_{13} = \frac{\beta_3 T_0}{A_{12}}, B_{14} = \frac{\gamma_3 C_0}{A_{12}}, B_{15} = \frac{A_{13}}{A_{12}}, B_{16} = \frac{\eta_{15}\psi_0 c_1\chi}{A_{12}}, B_{17} = \frac{A_{14}}{A_{12}},$$
$$B_{18} = \frac{\eta_{31}\psi_0 c_1\chi}{A_{12}}, B_{19} = \frac{\beta_1 T_0}{A_{12}}, B_{10} = \frac{\gamma_1 C_0}{A_{12}}, B_{20} = \frac{A_{15}}{A_{12}}, B_{21} = \frac{A_{16}\psi_0 c_1\chi}{A_{12}},$$
$$\varepsilon_1 = \frac{K_3}{K_1}, \varepsilon_2 = \frac{\beta_1}{\chi K_1}, \varepsilon_3 = \frac{\beta_3}{\chi K_1}, \varepsilon_4 = \frac{aC_0}{\chi K_1}, \varepsilon_5 = \frac{p_3 c_1\psi_0}{K_1}, \varepsilon_6 = \frac{D_3'}{D_1'}, \varepsilon_7 = \frac{\gamma_1}{bC_0}, \varepsilon_8 = \frac{\gamma_3}{bC_0},$$
$$\varepsilon_9 = \frac{aT_0}{bC_0}, \varepsilon_{10} = \frac{b_3\psi_0}{bC_0}, \varepsilon_{11} = \varepsilon_6\varepsilon_7, \varepsilon_{12} = \varepsilon_6\varepsilon_8, \varepsilon_{13} = \varepsilon_6\varepsilon_9, \varepsilon_{14} = \varepsilon_6\varepsilon_{10}, \varepsilon_{15} = \frac{1}{D_1' b\chi},$$
$$d_1 = \frac{\eta_{15}\eta_{33}}{A_{12}}, d_2 = \frac{\in_{11} c_1\psi_0\chi\eta_{33}}{A_{12}}, d_3 = \frac{\eta_{31}\eta_{33}}{A_{12}}, d_4 = \frac{\eta_{33}^2}{A_{12}}, d_5 = \frac{\in_{33} c_1\psi_0\chi\eta_{33}}{A_{12}}, d_6 = \frac{p_3 T_0\eta_{33}}{A_{12}}, d_7 = \frac{b_3 C_0\eta_{33}}{A_{12}},$$
$$h_1 = \frac{\eta_{15}}{A_{12}}, h_2 = \frac{\eta_{33}}{A_{12}}, h_3 = \frac{A_{16}}{A_{12}}, h_4 = \frac{\in_{11}\psi_0 c_1\chi}{A_{12}}, h_5 = \frac{\in_{33}\psi_0 c_1\chi}{A_{12}}, h_6 = \frac{p_3 T_0}{A_{12}}, h_7 = \frac{b_3 C_0}{A_{12}}.$$

5 PLANE WAVE SOLUTION AND REFLECTION PHENOMENA

Solution of the problem is now sought in the form of the harmonic travelling waves:

$$(u, w, \phi, \theta, \psi, c) = (\bar{u}, \bar{w}, \bar{\phi}, \bar{\theta}, \bar{\psi}, \bar{c}) \exp\{\iota k (-z \cos\theta + x \sin\theta) - \iota\omega t\}, \tag{29}$$

where k is the wave number, ω is angular frequency connected by the relation $\omega = kv$, v being the phase velocity and $(\sin\theta, \cos\theta)$ denotes the projection of wave normal of incident wave onto the xz-plane. Barred quantities are independent of x, z and t.

Injecting Eq. (29) into Eqs. (21)-(24) and Eqs. (27)-(28), we get the following set of six homogeneous equations in $\bar{u}, \bar{w}, \bar{\phi}, \bar{\theta}, \bar{\psi}, \bar{c}$

$$(F_{11}v^2 - F_{12})\bar{u} + F_{13}\bar{w} + F_{14}\bar{\psi} - F_{15}v\,\bar{\theta} - F_{16}v\bar{c} = 0, \tag{30}$$

$$F_{21}\bar{u} + (F_{11}v^2 - F_{23})\bar{w} - F_{24}\bar{\psi} + F_{25}v\,\bar{\theta} + F_{26}v\bar{c} = 0, \tag{31}$$

$$F_{31}v\bar{u} - F_{32}v\bar{w} + F_{33}v\,\bar{\psi} + F_{34}v^2\bar{\theta} - F_{35}\bar{\phi} + F_{36}v^2\bar{c} = 0, \tag{32}$$

$$F_{41}\bar{u} - F_{42}\bar{w} - F_{43}\bar{\psi} + F_{44}v\,\bar{\theta} + (F_{45}v^3 - F_{46}v)\bar{c} = 0, \tag{33}$$

$$F_{61}\bar{u} - F_{62}\bar{w} + F_{63}\bar{\psi} - F_{64}v\,\bar{\theta} - F_{65}v\bar{c} = 0, \tag{34}$$

$$(v^2 + F_{51})\bar{\phi} - v^2\bar{\theta} = 0. \tag{35}$$

The condition for the existence of non-trivial solution of the system of equations provides us

$$v^8 + Av^6 + Bv^4 + Cv^2 + D = 0, \tag{36}$$

where A, B, C and D are defined in Appendix A.

Using the transformation $v^2 = \zeta$ in Eq. (36), we obtain

$$\zeta^4 + A\zeta^3 + B\zeta^2 + C\zeta + D = 0. \tag{37}$$

The auxiliary equation corresponding to Eq. (37) is biquadratic in $\zeta = v^2$ with complex coefficients. The complex coefficient implies that four roots of this equation are complex and hence the four waves in the medium are attenuating waves. The complex phase velocity $v_i\ (i = 1, 2, 3, 4)$ of each wave can be resolved into propagation velocity $V_i\ (i = 1, 2, 3, 4)$ and attenuation coefficient $Q_i^{-1}\ (i = 1, 2, 3, 4)$. For a coupled wave with complex velocity $v_i = v_{iR} + v_{iI}$, define $V_i = (v_{iR}^2 + v_{iI}^2)/v_{iR}$ and $Q_i^{-1} = -2v_{iI}/v_{iR}$ as its phase velocity and attenuation coefficient respectively, where the letters R and I in the subscript denote the real and imaginary parts. The same direction of propagation and attenuation of these waves makes them homogeneous waves.

We assume that a set of coupled quasi waves (P_0) of amplitude A_0 propagating with the phase velcoity V_1 becomes incident obliquely at the surface, making an angle θ_0 with the normal. In order to satisfy the boundary conditions, we predicate that this incident P_0 wave gives rise to four reflected coupled quasi plane waves, namely, qP (quasi-P), $qM\ D$ (quasi mass diffusion), qT (quasi thermal) and qSV (quasi-SV) waves denoted by $P_{1,2,3,4}$ making angles $\theta_{1,2,3,4}$ respectively, with the normal as shown in Fig. 1.

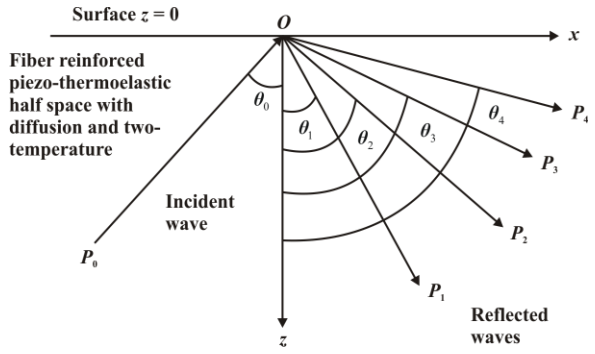

Fig.1
Schematic diagram of the problem showing incident and reflected waves.

The full structure of the wave field consisting of the incident and reflected waves, can be written as:

$$\left(w, u, \phi, \theta, c, \psi\right) = \left(1, a_1^*, b_1^*, c_1^*, d_1^*, e_1^*\right) A_0 P_0^- + \sum_{i=1,2,3,4} \left(1, a_i^*, b_i^*, c_i^*, d_i^*, e_i^*\right) A_i P_i^+, \tag{38}$$

where $P_o^- = \exp\left\{\iota k_1 \left(-z\cos\theta_0 + x\sin\theta_0\right) - \iota\omega_1 t\right\}$, is the phase factor of the incident wave at angle θ_0 with A_0 as amplitude constant, $P_i^+ = \exp\left\{\iota k_i \left(z\cos\theta_i + x\sin\theta_i\right) - \iota\omega_i t\right\}$, $\left(i = 1, 2, 3, 4\right)$ are the phase factors of the reflected waves corresponding to amplitude constants A_i at angles θ_i and $a_i^*, b_i^*, c_i^*, d_i^*$ and e_i^* are the coupling parameters as mentioned below:

$$a_i^* = -\frac{\left(H_{22}V_i^3 - H_{23}V_i\right) + \left(H_{24}V_i^2 + H_{25}\right)b_i^*}{H_{21}V_i}, \quad b_i^* = -\frac{I_{21}V_i^5 + I_{22}V_i^3 + I_{23}V_i}{I_{24}V_i^4 + I_{25}V_i^2 + I_{26}},$$

$$c_i^* = \frac{\left(V_i^2 + F_{51}\right)b_i^*}{V_i^2}, \quad d_i^* = \frac{G_{41}V_i a_i^* - G_{42}V_i + \left(G_{43}V_i^2 + G_{44}\right)b_i^*}{G_{45}V_i^2},$$

$$e_i^* = -\frac{F_{31}V_i a_i^* - F_{32}V_i + \left(F_{34}V_i^2 + F_{37}\right)b_i^* + F_{36}V_i^2 d_i^*}{F_{33}V_i}.$$

6 AMPLITUDE RATIOS AND ENERGY RATIOS

In order to determine the amplitude ratios and energy ratios of reflected waves, we will impose appropriate boundary conditions at the surface $z = 0$ of the considered half space. The boundary conditions are described as follows:

1. Mechanical boundary conditions that the surface of the half-space is traction free $\sigma_{zz} = \sigma_{zx} = 0$,
2. Thermal boundary condition that the surface of the half-space is isothermal $\phi = 0$,
3. Mass concentration boundary condition that the surface of the half-space is free from mass concentration $c = 0$.

The above boundary conditions are identically satisfied if and only if $k_1V_1 = k_2V_2 = k_3V_3 = k_4V_4$ and $k_1\sin\theta_1 = k_2\sin\theta_2 = k_3\sin\theta_3 = k_4\sin\theta_4$, which can further be written as (extended Snell's law) $\frac{\sin\theta_1}{V_1} = \frac{\sin\theta_2}{V_2} = \frac{\sin\theta_3}{V_3} = \frac{\sin\theta_4}{V_4}$.

Now, owing to boundary conditions with the help of aforementioned extended Snell's law and incorporating expressions of field variables from Eq. (38) into Eqs. (18) and (19), one can obtain the following system of simultaneous equations

$$A_{ij}Z_j = Y_i \ \left(i, j = 1, 2, 3, 4\right). \tag{39}$$

Here, $Z_{1,2,3,4}$ are the reflection coefficients (ratio of amplitudes of respective reflected waves to the amplitude of incident wave) of reflected $P_{1,2,3,4}$ waves given by $\frac{A_{1,2,3,4}}{A_0}$ and the entries A_{ij} 's and Y_i 's are defined below:

$$
\begin{aligned}
&A_{1j} = \iota B_{11} k_j \sin\theta_j a_j^* + \iota k_j \cos\theta_j + \iota B_{12} k_j \cos\theta_j e_j^* - B_{13} c_j^* - B_{14} d_j^*,\\
&A_{2j} = \iota B_{15} k_j \cos_j a_j^* + \iota B_{15} k_j \sin\theta_j + \iota B_{16} k_j \sin\theta_j e_j^*,\\
&A_{3j} = b_j^*, A_{4j} = d_j^*,\\
&Y_1 = -\iota B_{11} k_1 \sin\theta_0 a_1^* + \iota k_1 \cos\theta_0 + \iota B_{12} k_1 \cos\theta_0 e_1^* + B_{13} c_1^* + B_{14} d_1^*,\\
&Y_2 = \iota B_{15} k_1 \cos\theta_0 a_1^* - \iota B_{15} k_1 \sin\theta_0 - \iota B_{16} k_1 \sin\theta_0 e_1^*,\\
&Y_3 = -b_1^*, Y_4 = -d_1^*.
\end{aligned}
$$

Once all the reflected waves are determined, they should be validated to ensure that the energy of incident wave is equal to the energy sum of reflected waves, *i.e.*, the sum of energy flux component along the normal direction of the boundary should be conserved. At the surface $z = 0$, the distribution of energy among different reflected waves across a surface element of unit area is considered. The general expression of the wave energy flow is defined as (Following Kuang and Yuan [15]):

$$
P^* = -\sigma_{zz}\dot{w} - \sigma_{zx}\dot{u} + \psi\dot{D}_3 - K_{33}\phi_{,z}\frac{\phi}{T_0}. \tag{40}
$$

Now we calculate P^* for the incident and each of reflected waves and hence obtain the energy ratios giving the time rate of average energy transmission for the reflected waves to that of the incident wave. The expressions for these energy ratios E_i $(i = 1, 2, 3, 4)$ for reflected waves are given by

$$
E_i = \frac{\langle P_i^* \rangle}{\langle P_0^* \rangle}, \tag{41}
$$

where

$$
\langle P_i^* \rangle = \left(\iota\omega_i \left(A_{1i} + A_{2i} a_i^* - A_{5i} e_i^* \right) - \frac{K_{33}}{T_0} \iota k_i \cos\theta_i c_i^{*2} \right) Z_i^2 \quad \text{and} \quad \langle P_0^* \rangle = -\iota\omega_1 \left(Y_1 + Y_2 a_1^* + Y_5 e_1^* \right) + \frac{K_{33}}{T_0} \iota k_1 \cos\theta_0 c_1^{*2},
$$

where

$$
\begin{aligned}
&A_{5i} = \iota k_i \left(d_3 a_i^* \sin\theta_i + \left(d_4 - d_5 e_i^* \right) \cos\theta_i \right) + d_6 e_i^* + d_7 d_i^*, (i = 1, 2, 3, 4)\\
&Y_5 = \iota k_1 \left(d_3 a_1^* \sin\theta_0 + \left(-d_4 + d_5 e_1^* \right) \cos\theta_0 \right) + d_6 e_1^* + d_7 d_1^*
\end{aligned}
$$

and all other constants have been defined earlier. We note that these energy ratios also depend on the elastic properties of the medium, angle of incidence and amplitude ratios. The phenomena of conservation of the energy at the surface will be verified graphically in numerical results and discussion section.

7 PARTICULAR CASES

7.1 Neglecting diffusion effect

By taking $a = b = D_{ij} = \gamma_{ij} = b_i = 0$ in the governing equations and removing mass diffusion equation, the medium will be free from diffusion effect and then we shall be left with the relevant reflection problem in a piezo-

thermoelastic diffusive solid with two-temperature. In this case, the wave corresponding to diffusion *i.e. QMD* wave would not appear in the medium. Following the similar steps as in the general case, the velocities of these reflected waves will be obtained by the equation

$$\zeta'^{3} + A'\zeta'^{2} + B'\zeta' + C' = 0. \tag{42}$$

The roots of Eq. (42) give three values of $\zeta' = V'^{2}$ which correspond to three reflected coupled plane waves $P_{1,2,3}$, namely, *qP*, *qT* and *qSV* waves propagating with velocities $V'_{1,2,3}$ respectively and A', B' and C' are defined in Appendix B.

In this case, the boundary condition $c = 0$ will disappear and taking into consideration the remaining boundary conditions, reflection coefficients can be calculated from following set of equations

$$A'_{ij} Z'_j = Y'_i, (i, j = 1, 2, 3) \tag{43}$$

where $Z'_{1,2,3}$ are reflection coefficients corresponding to $P_{1,2,3}$ waves and other constants are defined in Appendix B.

7.2 Neglecting two-temperature effect

By setting $a_{11} = a_{33} = 0$ in governing equations, the two temperatures ϕ and θ will coincide and the problem will be reduced in a fiber reinforced piezo-thermoelastic diffusive medium. With these appropriate changes, phase velocities, reflection coefficients and energy ratios will be obtained from expressions (37), (39) and (41) correspondingly in the considered medium.

7.3 Neglecting piezoelectric effect

If the piezoelectric effect is removed from the thermoelastic medium, then we shall be dealing a half-space problem in a fiber reinforced termodiffusive medium with two-temperature. This can be achieved by substituting $\eta_{33} = \eta_{31} = \eta_{15} = \in_{11} = \in_{33} = p_3 = b_3 = 0$ and removing Gauss equation from the basic equations. Then the phase velocities of reflected waves are given by

$$\zeta^4 + P\zeta^3 + Q\zeta^2 + R\zeta + S = 0, \tag{44}$$

where $\zeta = V^2$ gives phase velocities $V_{1,2,3,4}$ of reflected quasi $P_{1,2,3,4}$ waves. The amplitude ratios of reflected waves are given by

$$B_{ij} Z_j = C_i, (i, j = 1, 2, 3, 4) \tag{45}$$

where $Z_{1,2,3,4}$ are amplitude ratios of reflected quasi $P_{1,2,3,4}$ waves. All other constants in above-mentioned two equations are defined in Appendix C.

If we further remove diffusion effect, then our results match with those of Deswal et al. [25] (removing rotation effect and making changes in the proposed theory.)

7.4 Isotropic case

In order to study the problem of wave propagation and reflection phenomena for an isotropic, piezo-thermoelastic medium with diffusion and two-temperature, it is sufficient to set the value of elastic parameters as $\alpha = \beta = \mu_L - \mu_T = 0$ in the governing equations and treating η_{ijk} as permutation tensor. If we also remove

piezoelectric effects in this case, then our results are in quite good agreement with those achieved by Bijarnia and Singh [44], by applying changes in the applied theory and boundary conditions.

8 NUMERICAL RESULTS AND DISCUSSION

With an aim to discuss the behaviour of wave propagation through a fiber reinforced transversely isotropic piezo-thermoelastic diffusive medium with two-temperature in greater detail, a numerical analysis is carried out. The numerical work has been carried out with the help of computer programming using the software MATLAB. For the purpose of numerical computation, the material constants of problem are taken as (Followig Abbas et al. [23]):

$$\lambda = 5.65\times10^{10}\ kgm^{-1}s^{-2},\ \mu_T = 2.46\times10^{10}\ kgm^{-1}s^{-2},\ \mu_L = 5.66\times10^{10}\ kgm^{-1}s^{-2},\ \alpha = -1.28\times10^{10}\ kgm^{-1}s^{-2},$$
$$\beta = 220.90\times10^{10}\ kgm^{-1}s^{-2},\ c_E = 0.787\times10^{3}\ Jkg^{-1}K^{-1},\ K_1 = 0.0921\times10^{3}\ Wm^{-1}K^{-1},$$
$$K_3 = 0.0963\times10^{3}\ Jm^{-1}K^{-1}s^{-1},\ \alpha_{11} = 0.017\times10^{-4}\ K^{-1},\ \alpha_{33} = 0.015\times10^{-4}\ K^{-1},\ \tau_0 = 0.02\,s,$$
$$\rho = 2660\ kgm^{-3},\ T_0 = 293\ K,\ a_{11} = 0.02m^2,\ a_{33} = 0.03m^2$$

Piezoelectric and diffusion parameters are taken as (Following Sharma et al. [14] and Kumar and Sharma [41]):

$$a = 1.2\times10^{4}m^2s^{-2}K^{-1},\ b = 0.9\times10^{6}m^5kg^{-1}s^{-2},\ D_1^{'} = 0.85\times10^{-8}kgsm^{-3},\ D_3^{'} = 0.8\times10^{-8}kgsm^{-3},$$
$$v_{11} = 1.98\times10^{-4}m^3kg^{-1},\ v_{33} = 1.9\times10^{-4}m^3kg^{-1},\ \tau^0 = 0.2s,\ \eta_{33} = 0.347Cm^{-2},\ \eta_{31} = -0.160Cm^{-2},$$
$$\eta_{15} = -0.138Cm^{-2},\ \in_{11} = 8.26\times10^{-11}C^2kg^{-1}m^{-3}s^2,\ \in_{33} = 9.03\times10^{-11}C^2kg^{-1}m^{-3}s^2,$$
$$p_3 = -2.94\times10^{-6}CK^{-1}m^{-2},\ \psi_0 = 10kgm^2s^{-2}C^{-1},\ b_3 = 0.5kg^{-1}Cm, C_0 = 10kgm^{-3}.$$

with these numerical values of the parameters, the values of different characteristics of reflected waves are computed and plotted graphically for the frequency $\omega = 10\ rad\ s^{-1}$. From application point of view, we have divided the plots in seven categories. In first category (Figs. 2(a-d)) and second category (Figs. 3(a-d)), we have depicted the variations of reflection coefficients and phase velocities respectively, by taking into account both the factors, namely, two-temperature parameter and piezoelectricity. Third category (Figs. 4(a-d)) and fourth category (Figs. 5(a-d)) exhibit the behaviour of reflection coefficients and phase velocities of reflected waves in transversely isotropic and isotropic medium. Fifth category (Figs. 6(a-d)) has been plotted to observe the variations of phase velocities when diffusion parameters are neglected from the medium considered. Sixth category (Figs. 7(a-d)) is meant to analyze the effects of incident angle and frequency on different reflection coefficients. This category elucidates three dimensional plots of reflection coefficients against angle of incidence $\left(0° < \theta_0 < 90°\right)$ and frequency $\left(1 \le \omega \le 10\right)$. Seventh category (Fig. 8) is plotted to exhibit the profiles of energy ratios with verification of energy conservation law in general case.

8.1 Category I

In Figs. 2 (a-d), we have examined the variations of amplitude ratios against angle of incidence for three different cases: (i) general case, (ii) without two-temperature and (iii) without piezoelectric effect. Fig. 2(a) is plotted for amplitude ratio $\left|Z_1\right|$. It is clear from the figure that in the general case and in the absence of two-temperature parameter, the curves of amplitude ratio $\left|Z_1\right|$ begin with their minimum value and then go on increasing gradually attaining maximum value unity near grazing incidence. However, the opposite scenario is observed in the absence of piezoelectric effects. The numerical values of Z_1 are enhanced a little in the presence of two-temperature while those are weakened in the presence of piezoelectricity.

Effects of two-temperature and piezoelectricity are quite pertinent on amplitude ratio $\left|Z_2\right|$ and can be noticed from Fig. 2(b). In all the three cases, amplitude ratio $\left|Z_2\right|$ starts with its maximum value and then diminishes to zero following a decreasing trend. In the general case and in the absence of piezoelectricity, amplitude ratio $\left|Z_2\right|$

decreases smoothly while in the absence of two-temperature, it decreases sharply. It is observed that the presence of two-temperature parameter diminishes the amplitude ratio $|Z_2|$ numerically. However, piezoelectricity exhibits mixed kind of effect. Piezoelectricity has an increasing effect upto $\theta_0 = 40°$ and a decreasing effect after $\theta_0 = 40°$ on amplitude ratio $|Z_2|$.

Fig. 2(c) depicts the variations of amplitude ratio $|Z_3|$. From the figure, it can be noted that the modulus of amplitude ratio Z_3 is maximum at 0° angle of incidence. It then decreases sharply and takes its minimum value zero near grazing incidence. It is also assessed that the amplitude ratio $|Z_3|$ shows similar pattern in the entire range of incident angle for all the three cases. However, dissimilarity lies on the ground of magnitude. Presence of two-temperature magnifies the values of amplitude ratio $|Z_3|$. The same observation holds for the piezoelectric effect.

The variation of modulus values of amplitude ratio Z_4 are illustrated in Fig. 2(d). Numerical values of Z_4 first increase from its minima (zero value) to maxima near $\theta_0 = 84°$ and then go on decreasing upto grazing incidence. The behaviour of amplitude ratio $|Z_4|$, for all the three cases, is alike with significant difference in their degree of sharpness. The effect of two-temperature is negligible for the amplitude ratio $|Z_4|$ whereas piezoelectricity has oscillatory effect on this amplitude ratio. The maximum impact zone of piezoelectricity is between $\theta_0 = 45°$ and $\theta_0 = 85°$.

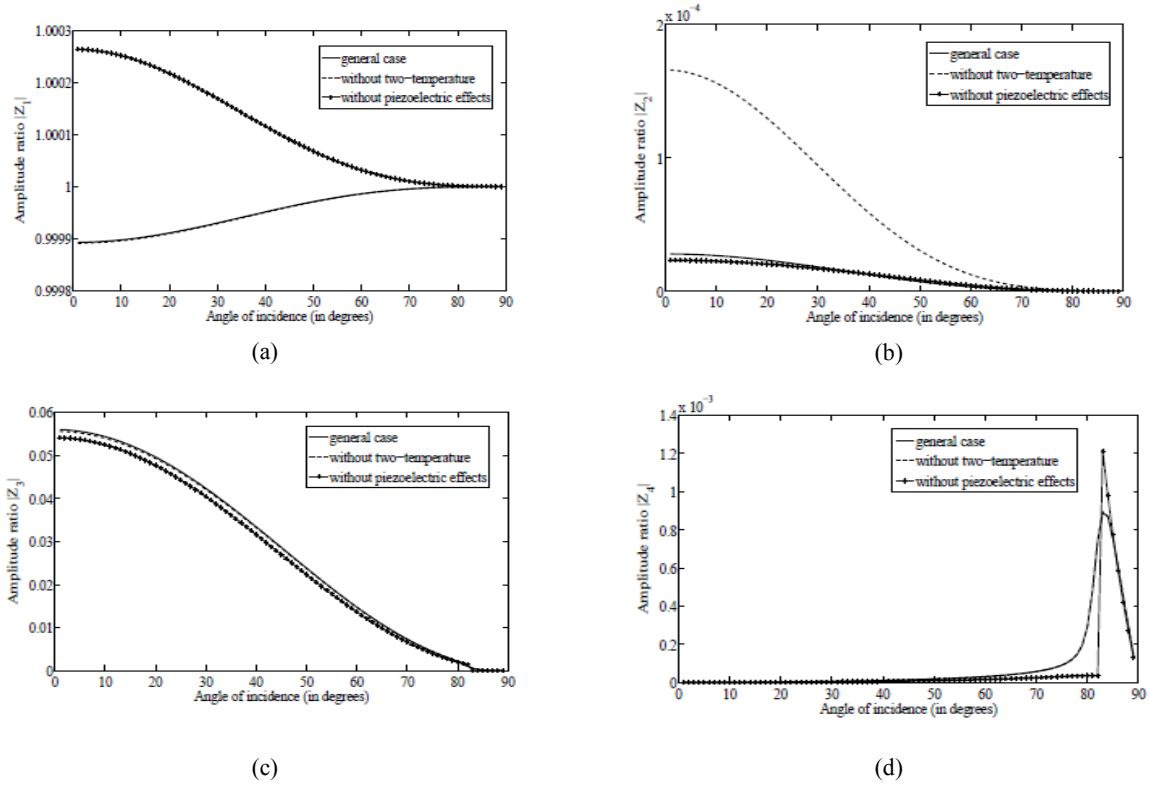

Fig.2
Variations of moduli of amplitude ratios of reflected waves to observe the effect of two-temperature and piezoelectricity.

8.2 Category II

To get acquainted with the effects of two-temperature and piezoelectricity on the phase velocities of reflected waves, we refer to Figs. 3 (a-d). Fig. 3(a) is plotted to display the variations of modulus of phase velocity V_1 of reflected *qP* wave versus angle of incidence. Phase velocity $|V_1|$ acts as an increasing function of angle of incidence in the whole

range of incident angle. This velocity begins with its minima near normal incidence and attains its maxima near grazing incidence in all the three cases. It can be noticed from the figure that numerical values of phase velocity $|V_1|$ are greater in the general case as compared to those in the absence of piezoelectric effect. Thus piezoelectricity causes an increasing effect on $|V_1|$. The effect of two-temperature seem to be negligible on $|V_1|$ as the curves of $|V_1|$ seem to coincide in the presence and absence of two-temperature. The small difference between absolute values of this velocity profile in the two cases exhibit the little impact of two-temperature.

Fig. 3(b) is plotted with the purpose to show the change in phase velocity $|V_2|$ of reflected *qMD* wave with angle of incidence. Phase velocity $|V_2|$ attains its maximum value near $\theta_0 = 0°$ and then goes on decreasing uniformly with angle of incidence, in all the three considered cases. Here Piezoelectricity has no effect on phase velocity $|V_2|$. However, two-temperature acts as an increasing agent for the velocity $|V_2|$ of reflected *qMD* wave.

Fig. 3(c) gives information about the profile of phase velocity $|V_3|$ which corresponds to reflected qT wave. As indicated in the figure, trends of phase velocity $|V_3|$ are similar in nature in the entire range with significant difference in their magnitudes. The velocity decreases with increase in the angle of incidence. It is evident from the figure that two-temperature has an increasing effect on phase velocity $|V_3|$. The information is reversed for the piezoelectric effects.

The effects of two-temperature and piezoelectricity on modulus values of phase velocity V_4 have been shown in Fig. 3(d). First the velocity increases from its minima to maxima attaining maximum value near $\theta_0 = 72°$ and then decreases from maxima to minima. The profile is similar in all the three cases, having dissimilarity on the basis of magnitude and degree of sharpness of curves. In the absence of piezoelectricity, it increases more rapidly as compared to the presence of piezoelectricity. Piezoelectricity acts to decrease the phase velocity $|V_4|$ while two-temperature has negligible effect on the velocity profile.

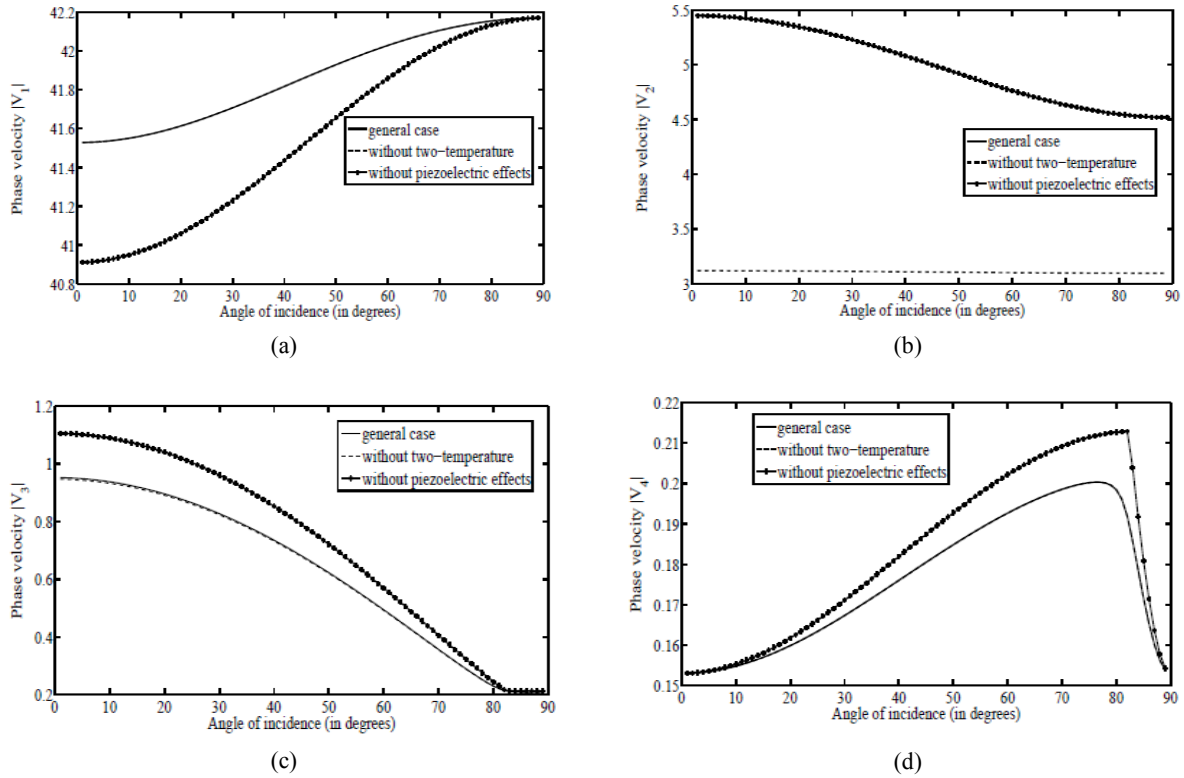

Fig.3
Variations of moduli of phase velocities of reflected waves to observe the effect of two-temperature and piezoelectricity.

8.3 Category III

In order to exhibit the effect of anisotropy, the variations of amplitude ratios with angle of incidence of coupled longitudinal quasi wave for two different cases (transversely isotropic medium and isotropic medium) are expressed in Figs. 4(a-d). The solid line corresponds to transversely isotropic medium (general case) and dashed line is corresponding to isotropic medium. Figs. 4(a-b) describe profiles of amplitude ratios $|Z_1|$ and $|Z_2|$ respectively. Fig. 4(a) depicts that in both the cases, modulus values of Z_1 increase in a similar fashion with the increase in angle of incidence, but at different rates. Amplitude ratio $|Z_1|$ rises at larger rate in the presence of anisotropy. Moreover, anisotropy acts to contract the numerical values of amplitude ratio Z_1 in the range $0° < \theta_0 \leq 62°$ and enhances in the remaining range. From the plot 4(b), we observe that in both the media, amplitude ratio $|Z_2|$ begins with its maximum values and then starts falling with different rates. In the transversely isotropic case, the amplitude ratio falls at larger rate. Presence of anisotropy magnifies amplitude ratio $|Z_2|$ before $\theta_0 = 68°$ and minifies after $\theta_0 = 68°$.

Anisotropy has pronounced effect on the amplitude ratios $|Z_3|$ and $|Z_4|$ also. Fig. 4(c) is characterizing that amplitude ratio $|Z_3|$ goes on decreasing with increment in the angle of incidence, in the presence and absence of anisotropy. The main difference is that it diminishes smoothly in the isotropic case while it diminishes sharply in the transversely isotropic case. The absence of anisotropy acts to lower down the curve of $|Z_3|$ before $\theta_0 = 34°$ and elevates the curve after $\theta_0 = 34°$. Fig. 4(d) emphasizes that amplitude ratio $|Z_4|$ is zero near normal incidence and non zero near grazing incidence, in both the cases. However, anisotropy obeys mixed kind of effect on this amplitude ratio.

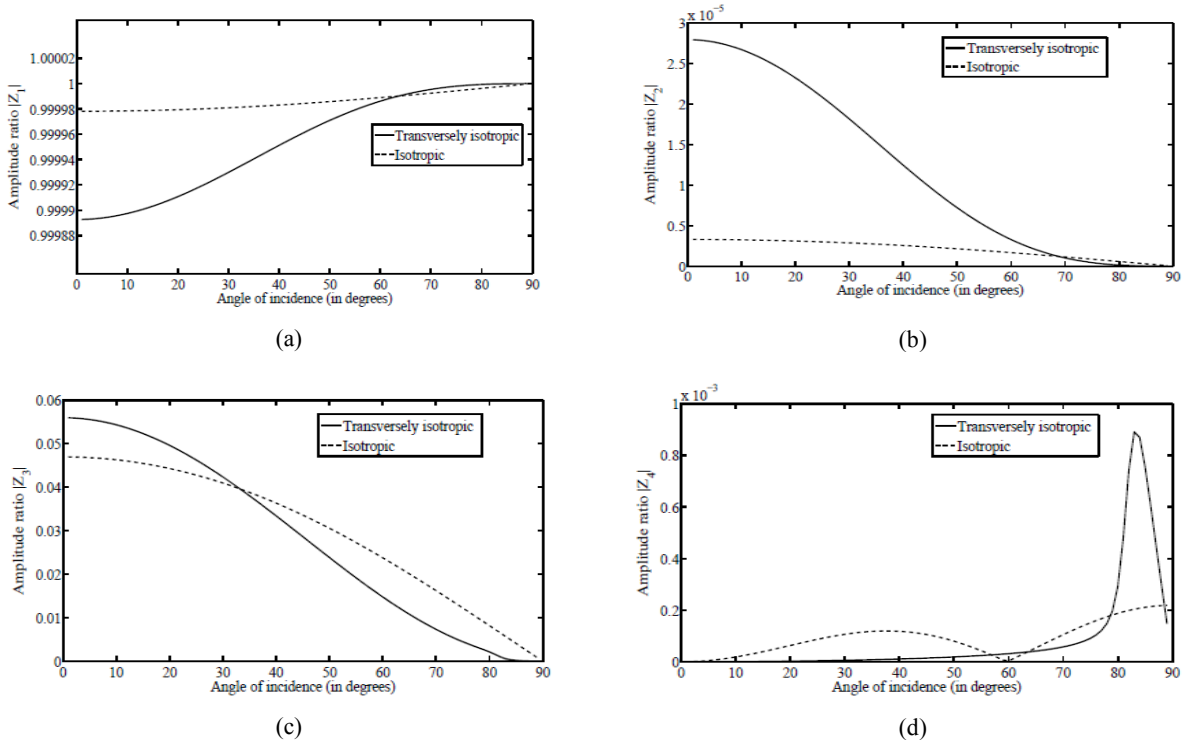

Fig.4
Variations of moduli of amplitude ratios of reflected waves to observe the effect of anisotropy.

8.4 Category IV

Figs. 5 (a-d) take into account the effect of anisotropy on phase velocities of reflected waves in the following media:

i. Transversely isotropic medium
ii. Isotropic medium

In the considered medium, z axis is the axis of symmetry so that the material properties are same in all the directions within the plane perpendicular to the axis, therefore the medium is transversely isotropic and phase velocities of reflected waves will vary with the direction of propagation of incident wave. The medium is elastically isotropic when there are no preferred directions in the medium. In that case, phase velocities of reflected waves will be independent of incident angle.

In all the figures of this set, the dashed curves are constant lines while the smooth ones vary with incident angle manifesting the effect of anisotropy, as solid curves correspond to the profiles of phase velocities in transversely isotropic medium while dashed curves are phase velocities in isotropic medium. From the plot 5(b), we observe that numerical values of phase velocity V_2 of reflected *qMD* wave are larger in the case of transversely isotropic medium in comparison to the isotropic medium while an opposite scenario is observed for phase velocities $|V_1|$, $|V_3|$ and $|V_4|$ of reflected *qP*, *qT* and *qSV* waves in Figs. 5(a), (c) and (d) respectively. Thus anisotropy gives rise to the values of phase velocity of reflected *qMD* wave while minifies to those of reflected *qP*, *qT* and *qSV* waves.

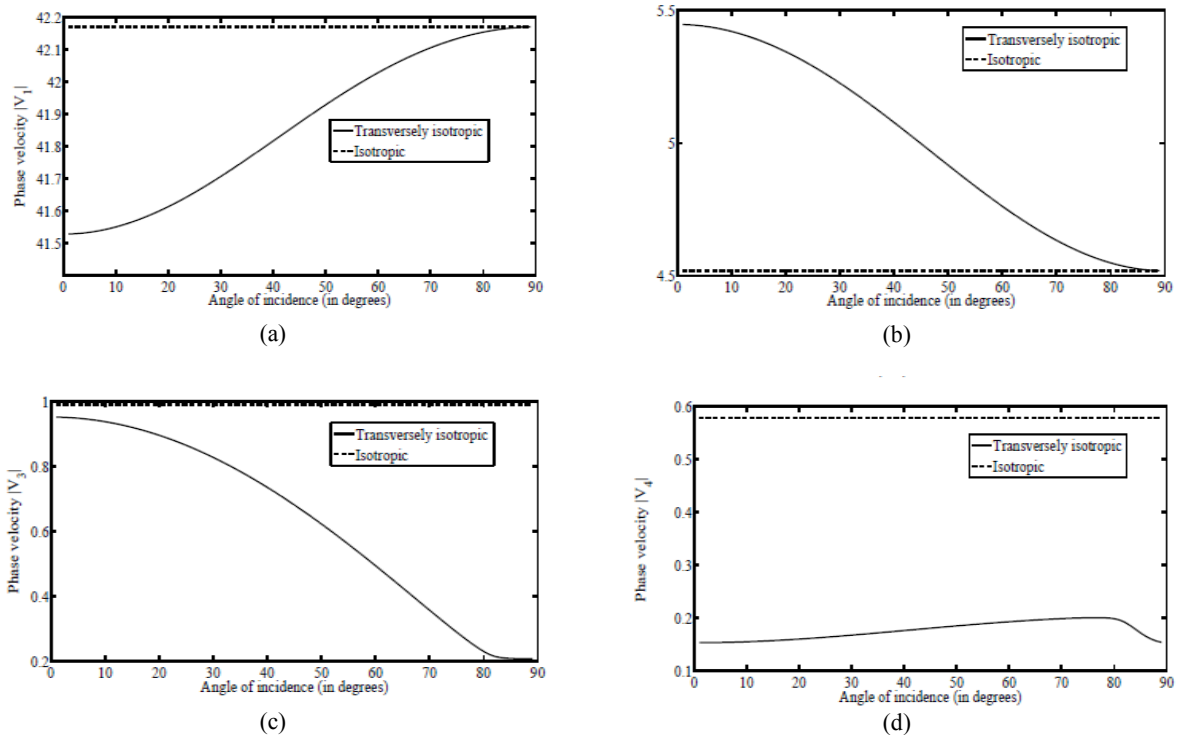

Fig.5
Variations of moduli of phase velocities of reflected waves to observe the effect of anisotropy.

8.5 Category V

Figs. 6(a-d) are plotted to demonstrate the variations of phase velocities of reflected waves under two different models, namely, with and without diffusion. In Fig. 6(a), we have elucidated the pattern of variation of phase velocities $|V_1|$ and $|V_1'|$ corresponding to *qP* wave in the presence and absence of diffusion respectively. Phase velocity obeys an increasing pattern in the presence of diffusion while a decreasing pattern in the absence of diffusion with increase in the angle of incidence which may not be very much clear from the figure as difference in the numerical values of the two velocities is very large. The values of phase velocity are found to be small in magnitude in the absence of diffusion which clearly points out that the diffusion parameters have appreciably increased the magnitude of phase velocity of *qP* wave.

In Fig. 6(b), we have plotted the modulus of phase velocity corresponding to reflected *qMD* wave as a function of angle of incidence. In this figure, we have only one curve of phase velocity $|V_2|$ corresponding to the presence of diffusion, because in the absence of diffusion, the quasi mass diffusion wave (*qMD*) will disappear from the medium. Presence of diffusion displays significant effect on phase velocity $|V_3|$ of reflected *qT* wave. Fig. 6(c) notifies that the phase velocity goes on decreasing upto $\theta_0 = 85°$, in both the cases. After that, the curve $|V_3|$ becomes zero while the curve $|V_2'|$ moves upward and becomes stationary. Diffusion causes an increasing effect on this phase velocity except in the range $86° \le \theta_0 < 90°$. Fig. 6(d) points out that in both the cases, velocities of reflected *qSV* wave follow similar kind of trend against angle of incidence with difference in their rate of rise and fall. Moreover, diffusion parameters lower down this phase velocity in the range $0° < \theta_0 \le 86°$ and elevate it after $\theta_0 = 86°$.

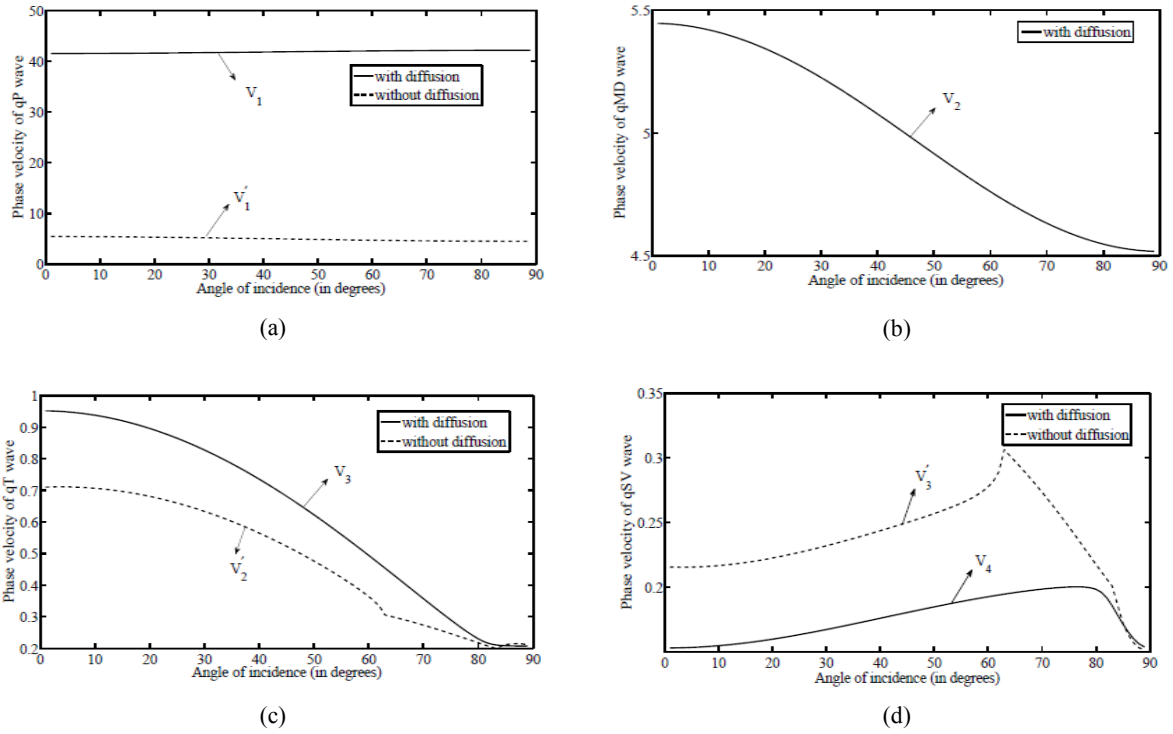

Fig.6
Variations of moduli of phase velocities of reflected waves in the presence and absence of diffusion.

8.6 Category VI

Figs. 7 (a-d) provide the three dimensional plots of amplitude ratios of reflected waves against frequency and incident angle as amplitude ratios depend upon angle of incidence as well as on the frequency of incident wave. The range of frequency and incident angle is taken as $1 \le \omega \le 10$ and $0° < \theta_0 < 90°$ respectively. Fig. 7(a) indicates that an increase in the values of frequency increases the amplitude ratio $|Z_1|$ of reflected *qP* wave. Similarly the angle of incidence causes an increasing effect on the profile of amplitude ratio $|Z_1|$, no matter what the value of frequency is in the considered range. Further $|Z_1|$ remains in the neighbourhood of unity for all the considered values of frequency and angle of incidence.

Fig. 7(b) reveals the fact that the profile of amplitude ratio $|Z_2|$ is similar for all the values of frequency. Figure indicates that frequency has a decreasing effect on the amplitude ratio $|Z_2|$ of reflected *qMD* wave. It means the

higher is the frequency, the lower are the values of $|Z_2|$. In the same way, angle of incidence also causes a decreasing effect on $|Z_2|$. Similar observation is noticed for amplitude ratio $|Z_3|$ from Fig. 7(c). Both frequency and angle of incidence have remarkable effect on amplitude ratio $|Z_4|$. Before $\theta_0 = 80°$, frequency has mixed kind of effect on amplitude ratio $|Z_4|$ and after $\theta_0 = 80°$, $|Z_4|$ enjoys decreasing effect of angular frequency. Numerical values of Z_4 first increase from its minima (zero value) to maxima near $\theta_0 = 80°$ and then go on decreasing upto grazing incidence. Thus angle of incidence obeys oscillatory effect on amplitude ratio $|Z_4|$.

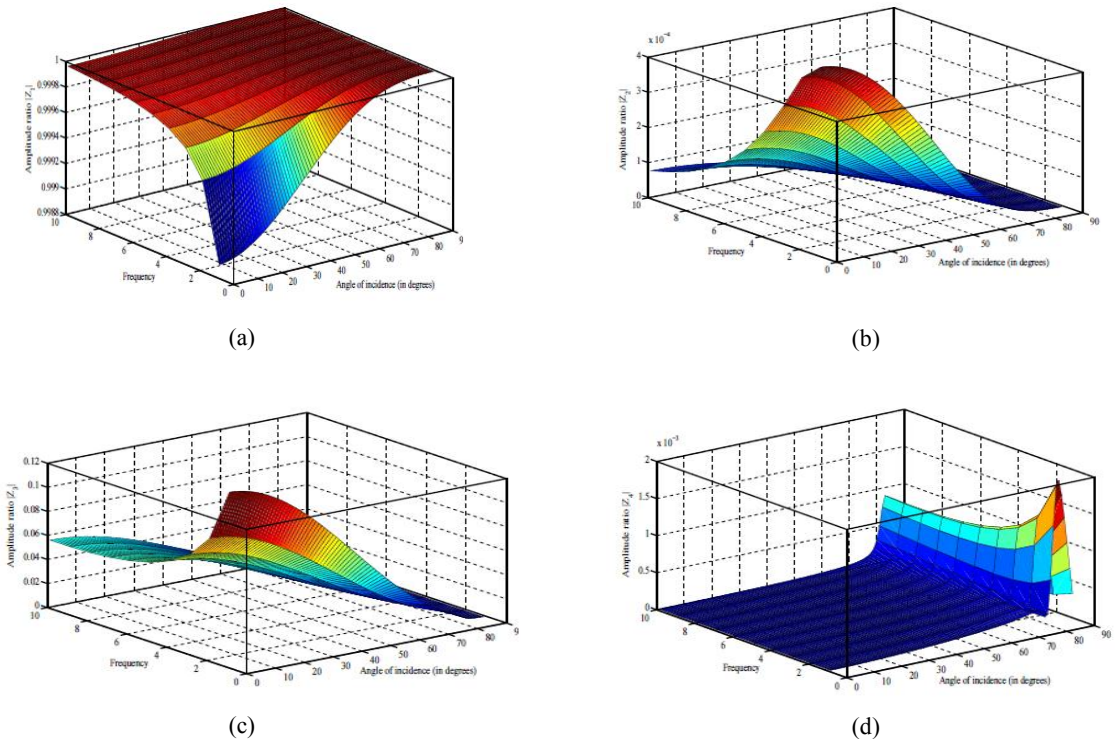

Fig.7
3D plot of amplitude ratios against frequency and angle of incidence.

8.7 Category VII

Fig. 8 depicts the variations of modulus of energy ratios of reflected waves with the angle of incidence of coupled longitudinal wave propagating with velocity V_1. Value of energy ratio $|E_1|$ remains approximately equal to unity, irrespective of the variations of angle of incidence. The energy ratios $|E_2|$, $|E_3|$and $|E_4|$ corresponding to the waves with speeds V_2, V_3 and V_4 are so small as compared to the energy ratio $|E_1|$ corresponding to the wave traveling with speeds V_1, that we have drawn each of them by mounting up their original values by 10^6, 10^8 and 10^{11} respectively. The energy ratios $|E_2|$ and $|E_3|$ behave like decreasing functions throughout the whole range of θ_0. The energy ratio $|E_4|$ is approximately zero upto $\theta_0 = 77°$, increases with increasing angle of incidence till $\theta_0 = 82°$ and then decreases in rest of the range. In the calculation of energy ratios, it has also been verified that the sum of energy ratios is equal to unity for each angle of incidence. In graphical representation also, $\sum_{i=1}^{4}|E_i| \approx 1$ at each angle of incidence, illuminating the fact that there is no loss of energy during reflection of waves.

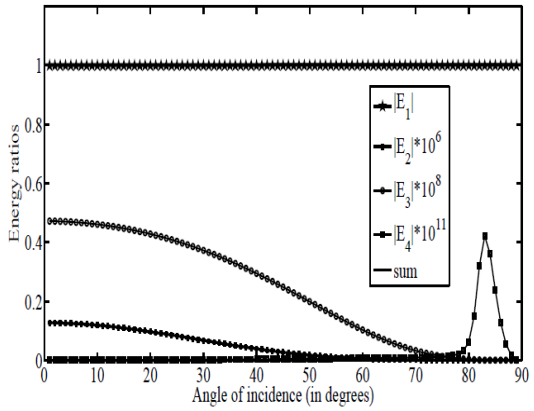

Fig.8
Variations of modulus of energy ratios against angle of incidence.

9 CONCLUSIONS

In the present model, we have explored the possibility of plane wave propagation in a fiber reinforced piezo-thermoelastic diffusive medium with two-temperature. From the analysis of the illustrations, we can arrive at the following conclusions:

- Piezoelectricity has a salient effect on all the reflection coefficients of reflected waves which can be readily seen from Figs. 2(a-d).
- Two-temperature parameter has pronounced effect on all the reflection coefficients and phase velocities. Behaviour of all the amplitude ratios and phase velocities is similar having dissimilarity in numerical values in the presence and absence of two-temperature parameter.
- Presence of piezoelectric effect is playing a vital role in all the physical quantities. Its presence diminishes the magnitudes of velocity $|V_3|$ and $|V_4|$ and increases the velocity $|V_1|$. However it shows negligible impact on phase velocity $|V_2|$.
- Another important phenomena observed is that phase velocities of all the reflected waves are constant in the absence of anisotropy which is physically reasonable as material properties are independent of direction in an isotropic medium.
- It is found that four waves vibrate with different phase velocities in a two-temperature fiber reinforced piezo-thermoelastic diffusive medium. The number of reflected waves reduces to three in the absence of diffusion as *qMD* wave will disappear in that case which is righteous from the physical standpoint.
- All the reflection coefficients $|Z_i|\,(i=1,2,3,4)$ are remarkably influenced by angular frequency. Increase in the values of angular frequency acts to increase the reflection coefficient $|Z_1|$ while decrease reflection coefficients $|Z_2|$ and $|Z_3|$. It has both decreasing and increasing effects on reflection coefficient $|Z_4|$.
- It is worth to observe that during whole range of incidence of set of coupled longitudinal wave of speed V_1, sum of the modulus values of energy ratios is approximately unity, thus proving the law of conservation of energy.

A significant number of both natural and man-made piezoelectric materials such as barium titanate, quartz, and PZT are available, which have myriads of applications such as manufacture of transducers, sensors, actuators, ultrasonic motors, resonators, microelectromechanical systems (MEMS), just to name a few. However, these piezoelectric materials have certain deficiencies, such as low piezoelectric constants, high-specific acoustic impedance, and shape control (due to their weight). To overcome these inhibitions and to obtain improvised effective thermal and electrical properties in comparison to those of piezoelectric and pyroelectric materials, fiber reinforced piezo-thermoelastic materials have come to be of widespread use now-a-days. Enhanced mechanical, thermal and electrical properties can be attained by systematically adapting the most advantageous properties of the constituents of composite materials. Although studies on reflection at boundaries of piezoelectric and thermoelastic materials have been performed previously, the integration of piezo-thermoelastic fiber reinforced composite materials with thermodissusive properties, in this work provides a better and more realistic explanation of the actual phenomena. The findings of this study have vast applications in scientific and engineering fields which include

geophysics, mining in oil industries, nondestructive evaluation and earthquake engineering, etc. These applications include developing new and efficient smart composites with enhanced stability and control, wireless communication, signal processing and creating intelligent structures, e.g. transducers, actuators, resonators, etc. using piezo-thermoelastic fiber reinforced composite materials which can be used to detect the responses of a structure by measuring the electric charge, reduce excessive responses by applying additional electric or thermal forces, etc.

APPENDIX A

$$A=\frac{I_2}{I_1}, B=\frac{I_3}{I_1}, C=\frac{I_4}{I_1}, D=\frac{I_5}{I_1}$$

where

$$I_1=I_{11}I_{24}-I_{14}I_{21},\ I_2=I_{11}I_{25}+I_{12}I_{24}-I_{14}I_{22}-I_{15}I_{21},\ I_3=I_{11}I_{26}-I_{13}I_{24}+I_{12}I_{25}-I_{14}I_{23}-I_{16}I_{21}-I_{15}I_{22},$$
$$I_4=I_{12}I_{26}-I_{13}I_{25}-I_{15}I_{23}-I_{16}I_{22},\ I_5=-I_{13}I_{26}-I_{16}I_{23},\ I_{11}=H_{11}H_{22},\ I_{12}=H_{22}H_{12}-H_{13}H_{21}-H_{11}H_{23},$$
$$I_{13}=H_{21}H_{14}+H_{12}H_{23},\ I_{14}=H_{11}H_{24},\ I_{15}=H_{24}H_{12}+H_{11}H_{25}-H_{15}H_{21},\ I_{16}=H_{25}H_{12}-H_{16}H_{21},$$
$$I_{21}=H_{31}H_{22},\ I_{22}=H_{22}H_{32}+H_{33}H_{21}-H_{31}H_{23},\ I_{23}=H_{21}H_{34}-H_{32}H_{23},\ I_{24}=H_{31}H_{24}-H_{35}H_{21},$$
$$I_{25}=H_{24}H_{32}+H_{31}H_{25}-H_{36}H_{21},\ I_{26}=H_{25}H_{32}-H_{37}H_{21},$$
$$H_{11}=G_{11}G_{45},\ H_{12}=G_{12}G_{45}+G_{17}G_{41},\ H_{13}=G_{13}G_{45},\ H_{14}=G_{14}G_{45}-G_{17}G_{42},\ H_{15}=G_{15}G_{45}+G_{17}G_{43},$$
$$H_{16}=G_{16}G_{45}+G_{17}G_{44},\ H_{21}=G_{21}G_{45}+G_{26}G_{41},\ H_{22}=G_{22}G_{45},\ H_{23}=G_{23}G_{45}+G_{26}G_{42},$$
$$H_{24}=G_{24}G_{45}+G_{26}G_{43},H_{25}=G_{25}G_{45}+G_{26}G_{44},\ H_{31}=G_{41}G_{35},\ H_{32}=G_{31}G_{45}-G_{36}G_{41},H_{33}=G_{35}G_{42},$$
$$H_{34}=G_{32}G_{45}-G_{36}G_{42},H_{35}=G_{35}G_{43},\ H_{36}=G_{33}G_{45}+G_{35}G_{44}-G_{36}G_{43},H_{37}=G_{34}G_{45}-G_{36}G_{44},$$
$$G_{11}=F_{11}F_{24},\ G_{12}=F_{21}F_{14}-F_{12}F_{24},\ G_{13}=F_{14}F_{11},\ G_{14}=F_{24}F_{13}-F_{14}F_{23},\ G_{15}=F_{25}F_{14}-F_{15}F_{24},$$
$$G_{16}=F_{27}F_{14}-F_{17}F_{24},\ G_{17}=F_{26}F_{14}-F_{16}F_{24},\ G_{21}=F_{21}F_{33}+F_{31}F_{24},\ G_{22}=F_{11}F_{33},\ G_{23}=F_{23}F_{33}+F_{32}F_{24},$$
$$G_{24}=F_{25}F_{33}+F_{34}F_{24},\ G_{25}=F_{27}F_{33}+F_{37}F_{24},\ G_{26}=F_{26}F_{33}+F_{36}F_{24},\ G_{31}=F_{31}F_{43}+F_{41}F_{33},$$
$$G_{32}=F_{33}F_{42}+F_{43}F_{32},\ G_{33}=F_{34}F_{43}+F_{44}F_{33},\ G_{34}=F_{37}F_{43}+F_{47}F_{33},\ G_{35}=F_{33}F_{45},\ G_{36}=F_{33}F_{46}-F_{43}F_{36},$$
$$G_{41}=F_{31}F_{63}-F_{61}F_{33},\ G_{42}=F_{32}F_{63}-F_{62}F_{33},\ G_{43}=F_{33}F_{64}+F_{63}F_{34},\ G_{44}=F_{33}F_{66}+F_{63}F_{37},$$
$$G_{45}=-F_{33}F_{65}-F_{63}F_{36},$$
$$F_{17}=F_{15}F_{51},\ F_{27}=F_{25}F_{51},\ F_{37}=F_{34}F_{51}-F_{35},\ F_{47}=F_{44}F_{51},\ F_{66}=F_{64}F_{51},\ F_{11}=\omega^2,$$
$$F_{12}=\left(B_{15}\cos^2\theta+B_{17}\sin^2\theta\right)\omega^2,\ F_{13}=B_{20}\omega^2\cos\theta\sin\theta,\ F_{14}=B_{21}\omega^2\cos\theta\sin\theta,\ F_{15}=\iota B_{19}\omega\sin\theta,$$
$$F_{16}=\iota B_{10}\omega\sin\theta,\ F_{21}=B_{20}\omega^2\cos\theta\sin\theta,\ F_{23}=\left(\cos^2\theta+B_{15}\sin^2\theta\right)\omega^2,$$
$$F_{24}=\left(B_{22}\cos^2\theta+B_{16}\sin^2\theta\right)\omega^2,\ F_{25}=\iota B_{13}\omega\cos\theta,\ F_{26}=\iota B_{14}\omega\cos\theta,\ F_{31}=iF_{34}\varepsilon_2\omega\sin\theta,$$
$$F_{32}=iF_{34}\varepsilon_3\omega\cos\theta,\ F_{33}=iF_{34}\varepsilon_5\omega\cos\theta,\ F_{34}=\iota\omega\left(1-\iota\omega\tau_0\right),\ F_{35}=\left(\varepsilon_1\cos^2\theta+\sin^2\theta\right)\omega^2,\ F_{36}=F_{34}\varepsilon_4,$$
$$F_{41}=\iota\left(\varepsilon_{11}\cos^2\theta+\varepsilon_{17}\sin^2\theta\right)\omega^3\sin\theta,\ F_{42}=\iota\left(\varepsilon_{12}\cos^2\theta+\varepsilon_8\sin^2\theta\right)\omega^3\cos\theta,$$
$$F_{43}=\iota\left(\varepsilon_{14}\cos^2\theta+\varepsilon_{10}\sin^2\theta\right)\omega^3\cos\theta,\ F_{44}=\left(\varepsilon_{13}\cos^2\theta+\varepsilon_9\sin^2\theta\right)\omega^2,\ F_{45}=\iota\omega\varepsilon_{15}\left(1-\iota\omega\tau^0\right),$$
$$F_{46}=\left(\varepsilon_6\cos^2\theta+\sin^2\theta\right)\omega^2,F_{51}=\left(a_{33}\cos^2\theta+a_{11}\sin^2\theta\right)\omega^2,\ F_{61}=h_3\omega^2\cos\theta\sin\theta,$$
$$F_{62}=\left(h_2\cos^2\theta+h_1\sin^2\theta\right)\omega^2,\ F_{63}=\left(h_5\cos^2\theta+h_4\sin^2\theta\right)\omega^2,\ F_{64}=\iota h_6\omega\cos\theta,\ F_{65}=\iota h_7\omega\cos\theta.$$

APPENDIX B

$$A'=\frac{I_2}{I_1},\ B'=\frac{I_3}{I_1},\ C'=\frac{I_4}{I_1},$$

$I_1 = H_{13}H_{21}$, $I_2 = H_{11}H_{24} + H_{13}H_{22} - H_{14}H_{21}$, $I_3 = H_{12}H_{23} + H_{11}H_{24} - H_{15}H_{21} - H_{14}H_{22}$,
$I_4 = H_{12}H_{24} - H_{15}H_{22}$,
$H_{11} = G_{11}G_{32}$, $H_{12} = G_{13}G_{31} + G_{12}G_{32}$, $H_{13} = G_{11}G_{33}$, $H_{14} = G_{14}G_{31} - G_{12}G_{33} - G_{11}G_{34}$, $H_{15} = G_{15}G_{31} - G_{12}G_{34}$,
$H_{21} = G_{22}G_{31}$, $H_{22} = G_{23}G_{31} + G_{21}G_{32}$, $H_{23} = G_{24}G_{31} - G_{21}G_{33}$, $H_{24} = G_{25}G_{31} - G_{21}G_{34}$,
$G_{11} = F_{11}F_{63}$, $G_{12} = -F_{14}F_{61} - F_{12}F_{63}$, $G_{13} = F_{13}F_{63} + F_{14}F_{62}$, $G_{14} = F_{14}F_{64} - F_{15}F_{63}$, $G_{15} = F_{14}F_{66} - F_{17}F_{63}$,
$G_{21} = F_{21}F_{63} + F_{24}F_{61}$, $G_{22} = F_{11}F_{63}$, $G_{23} = -F_{24}F_{62} - F_{23}F_{63}$, $G_{24} = F_{25}F_{63} - F_{24}F_{64}$, $G_{25} = F_{27}F_{63} - F_{24}F_{66}$,
$G_{31} = F_{31}F_{63} - F_{61}F_{33}$, $G_{32} = F_{32}F_{63} - F_{62}F_{33}$, $G_{33} = F_{33}F_{64} + F_{63}F_{34}$, $G_{34} = F_{37}F_{63} + F_{66}F_{33}$,
$F_{11,\,2,\,3,\,4,\,5,\,7}$, $F_{21,\,3,\,4,\,5,\,7}$, $F_{31,\,2,3,4,7}$ and $F_{61,\,2,\,3,\,4,\,6}$ are same as defined in Appendix A.
$A'_{1j} = \iota B_{11}k_j \sin\theta_j a_j^{*'} + \iota k_j \cos\theta_j + \iota B_{12}k_j \cos\theta_j e_j^{*'} - B_{13}c_j^{*'}$,
$A'_{2j} = \iota B_{15}k_j \cos\theta_j a_j^{*'} + \iota B_{15}k_j \sin\theta_j + \iota B_{16}k_j \sin\theta_j e_j^{*'}$, $A'_{3j} = b_j^{*'}$,
$Y_1' = -\iota B_{11}k_1 \sin\theta_0 a_1^{*'} + \iota k_1 \cos\theta_0 + \iota B_{12}k_1 \cos\theta_0 e_1^{*'} + B_{13}c_1^{*'}$,
$Y_2^{'} = \iota B_{15}k_1 \cos\theta_0 a_1^{*'} - \iota B_{15}k_1 \sin\theta_0 - \iota B_{16}k_1 \sin\theta_0 e_1^{*'}$, $Y_3' = -b_1^{*'}$,

where

$$a_j^{*'} = \frac{G_{32}V_j' - \left(G_{33}V_j'^2 + G_{34}\right)b_j^{*'}}{G_{31}V_j'},\ b_j^{*'} = -\frac{H_{21}V_j'^3 + H_{22}V_j'}{H_{23}V_j'^2 + H_{24}},\ c_j^{*'} = \frac{\left(V_j'^2 + F_{51}\right)b_j^{*'}}{V_j'^2},$$

$$e_j^{*'} = -\frac{F_{61}V_j'a_j^{*'} - F_{62}V_j' - \left(F_{64}V_j'^2 + F_{66}\right)b_j^{*'}}{F_{63}V_j'}(j = 1, 2, 3).$$

APPENDIX C

$P = \frac{I_2}{I_1}, Q = \frac{I_3}{I_1},\ R = \frac{I_4}{I_3}, S = \frac{I_5}{I_1}$,
$I_1 = H_{11}H_{24} - H_{14}H_{21}$, $I_2 = H_{11}H_{25} - H_{12}H_{24} - H_{14}H_{22} - H_{15}H_{21}$,
$I_3 = H_{11}H_{26} + H_{13}H_{24} - H_{12}H_{25} - H_{14}H_{23} - H_{16}H_{21} - H_{15}H_{22}$,
$I_4 = -H_{12}H_{26} + H_{13}H_{25} - H_{15}H_{23} - H_{16}H_{22}$, $I_5 = H_{13}H_{26} - H_{16}H_{23}$,
$H_{11} = G_{11}G_{22}$, $H_{12} = G_{12}G_{22} + G_{11}G_{23}$,
$H_{13} = G_{12}G_{23} - G_{13}G_{21}$, $H_{14} = G_{11}G_{24}$, $H_{15} = G_{14}G_{21} - G_{24}G_{12} + G_{11}G_{25}$,
$H_{16} = G_{15}G_{21} - G_{12}G_{25}, H_{21} = G_{22}G_{31}, H_{22} = G_{33}G_{21} - G_{23}G_{31} + G_{22}G_{32}$,
$H_{23} = G_{34}G_{21} - G_{23}G_2, H_{24} = G_{24}G_{31} - G_{21}G_{35}$,
$H_{25} = G_{24}G_{32} + G_{31}G_{25} - G_{36}G_{21}, H_{26} = G_{25}G_{32} - G_{37}G_{21}$,
$G_{11} = F_{11}F_{36}, G_{12} = F_{31}F_{16} - F_{12}F_{36}, G_{13} = F_{13}F_{36} - F_{16}F_{32}$,
$G_{14} = F_{15}F_{36} - F_{16}F_{34}, G_{15} = F_{17}F_{36} - F_{16}F_{37}, G_{21} = F_{21}F_{36} - F_{31}F_{26}$,
$G_{22} = F_{11}F_{36}, G_{23} = F_{23}F_{36} - F_{32}F_{26}, G_{24} = F_{25}F_{36} - F_{34}F_{26}$,
$G_{25} = F_{27}F_{36} - F_{37}F_{26}, G_{31} = F_{31}F_{45}, G_{32} = -F_{36}F_{41} - F_{46}F_{31}$,
$G_{33} = F_{32}F_{45}, G_{34} = F_{36}F_{42} + F_{46}F_{32}, G_{35} = F_{34}F_{45}$,
$G_{36} = F_{37}F_{45} - F_{46}F_{34} - F_{36}F_{44}, G_{37} = -F_{36}F_{47} - F_{37}F_{43}$,
$F_{11,\,2,\,3,\,5,\,6,\,7}$, $F_{21,\,2,\,3,\,5,\,6,\,7}$, $F_{31,\,2,\,3,\,6,\,7}$ and $F_{41,\,2,\,4,\,5,\,6,\,7}$ are same as defined in Appendix A.
$A_{1j} = \iota B_{11}k_j \sin\theta_j a_j^* + \iota k_j \cos\theta_j - B_{13}c_j^* - B_{14}d_j^*$,
$A_{2j} = \iota B_{15}k_j \cos\theta_j a_j^* + \iota B_{15}k_j \sin\theta_j$, $A_{3j} = b_j^*, A_{4j} = d_j^*$,
$Y_1 = -\iota B_{11}k_1 \sin\theta_0 a_1^* + \iota k_1 \cos\theta_0 + B_{13}c_1^* + B_{14}d_1^*$,

$$Y_2 = \iota B_{15} k_1 \cos\theta_0 a_1^* - \iota B_{15} k_1 \sin\theta_0,\ Y_3 = -b_1^*, Y_4 = -d_1^*,$$

$$a_j^* = -\frac{\left(G_{22}V_j^{\ 3} - G_{23}V_j\right) + \left(G_{24}V_j^{\ 2} + G_{25}\right)b_j^*}{G_{21}V_j},\ b_j^* = -\frac{H_{21}V_j^{\ 5} + H_{22}V_j^{\ 3} + H_{23}V_j}{H_{24}V_j^{\ 4} + H_{25}V_j^{\ 2} + H_{26}},\ c_j^* = \frac{\left(V_j^{\ 2} + F_{51}\right)b_j^*}{V_j^{\ 2}},$$

$$d_j^* = \frac{F_{32}V_j - F_{31}V_j a_j^* - \left(F_{34}V_j^{\ 2} + F_{37}\right)b_j^*}{F_{36}V_j^{\ 2}} \left(j = 1, 2, 3, 4\right).$$

REFERENCES

[1] Biot M.A., 1956, Thermoelasticity and irreversible thermodynamics, *Journal of Applied Physics* **27**: 240-253.

[2] Lord H.W., Shulman Y., 1967, A generalized dynamical theory of thermoelasticity, *Journal of the Mechanics and Physics of Solids* **15**: 299-309.

[3] Ignaczak J., Ostoja-Starzewski M., 2010, *Thermoelasticity with Finite Wave Speeds*, *Mathematical Monographs*, Oxford University Press, Oxford.

[4] Lata P., 2018, Reflection and refraction of plane waves in layered nonlocal elastic and anisotropic thermo-elastic medium , *Structural Engineering and Mechanics* **66**: 113-124.

[5] Lata P., 2018, Effect of energy dissipation on plane waves in sandwiched layered thermoelastic medium, *Steel and Composite Structures* **27**: 439-451.

[6] Lata P., Kaur I., 2019, Plane wave propagation in transversely isotropic magneto-thermoelastic rotating medium with fractional order generalized heat transfer, *Structural Monitoring and Maintenance-An International Journal* **6**: 191-218.

[7] Lata P., Kaur I., 2019, Thermomechanical interactions due to time harmonic sources in a transversely isotropic magneto thermoelastic solids with rotation, *International Journal of Microstructure and Materials Properties* **14**: 549-577.

[8] Mindlin R.D., 1961, *On the Equations of Motion of Piezoelectric Crystals*, Problems of Continuum Mechanics, N.I. Muskelishvili's Birthday 70, SIAM, Philadelphia **1961**: 282-290.

[9] Nowacki W., 1978, Some general theorems of thermo-piezoelectricity, *Journal of Thermal Stresses* **1**: 171-182.

[10] Nowacki W., 1979, *Foundations of Linear Piezoelectricity*, Parkus H., (Ed.), Electromagnetic Interactions in Elastic Solids, Springer, Wien, Chapter 1.

[11] Nowacki W., 1983, *Mathematical Models of Phenomenological Piezoelectricity*, New problems in Mechanics of Continua, University of Waterloo Press, Ontario **1983**: 29-49.

[12] Chandrasekharaiah D.S., 1984, A temperature rate dependent theory of piezoelectricity, *Journal of Thermal Stresses* **7**: 293-306.

[13] Chandrasekharaiah D.S., 1988, A generalized linear thermoelasticity theory of piezoelectric media, *Acta Mechanica* **71**: 39-49.

[14] Sharma J.N., Walia V., Gupta S.K., 2008, Reflection of piezothermoelastic waves from the charge and stress free boundary of a transversely isotropic half space, *International Journal of Engineering Science* **46**: 131-146.

[15] Kuang Z.B., Yuan X.G., 2011, Reflection and transmission of waves in pyroelectric and piezoelectric materials, *Journal of Sound and Vibration* **330**: 1111-1120.

[16] Yuan X., Jiang Q., 2016, Reflection of plane waves from rotating pyroelectric half-space under initial stresses, *Zeitschrift für Angewandte Mathematik und Mechanik* **97**: 365-374.

[17] Vashishth A.K., Sukhija H., 2015, Reflection and transmission of plane waves from fluid- piezothermo- elastic solid interface, *Applied Mathematics and Mechanics* **36**: 11-36.

[18] Othman M.I.A., Ahmed E.A.A., 2019, Exact analytical solution of a homogeneous anisotropic piezo- thermoelasic half-space of a hexagonal type under different fields with three theories, *Microsystem Technologies* **25**: 1423-1435.

[19] Pipkin A.C., 1973, *Finite Deformations of Ideal Fiber-Reinforced Composites*, Sendeckyj G.P., (Ed.), Composites Materials, Academic Press, New York **2**: 251-308.

[20] Rogers T.G., 1975, *Anisotropic Elastic and Plastic Materials*, Thoft Christensen P., (Ed.), Continuum Mechanics Aspects of Geodynamics and Rock Fracture Mechanics, Reidel, Dordrecht **1975**: 177-200.

[21] Belfield A.J., Rogers T.G., Spencer A.J.M., 1983, Stress in elastic plates reinforced by fiber lying in concentric circles, *Journal of the Mechanics and Physics of Solids* **31**: 25-54.

[22] Singh S.S., Tomar S.K., 2007, Shear waves at a corrugated interface between two dissimilar fiber reinforced elastic half spaces, *Journal of Mechanics of Materials and Structures* **2**: 167-188.

[23] Abbas I.A., Abd-Alla A.N., Othman M.I.A., 2011, Generalized magnetothermoelasticity in a fiber-reinforced anisotropic half-space, *International Journal of Thermophysics* **32**: 1071-1085.

[24] Said S.M., Othman M.I.A., 2016, Effects of gravitational and hydrostatic initial stress on a two-temperature fiber-reinforced thermoelastic medium for three-phase-lag, *Journal of Solid Mechanics* **8**: 806-822.

[25] Deswal S., Sheokand S.K., Kalkal K.K., 2019, Reflection at the free surface of fiber-reinforced thermoelastic rotating medium with two-temperature and phase-lag, *Applied Mathematical Modelling* **65**: 106-119.
[26] Lata P., Kaur I., 2020, Thermomechanical interactions in transversely isotropic magneto-thermoelastic medium with fractional order generalized heat transfer and hall current, *Arab Journal of Basic and Applied science* **27**: 13-26.
[27] Chen P.J., Gurtin M.E., 1968, On a theory of heat conduction involving two temperatures, *Zeitschrift für Angewandte Mathematik und Physik* **19**: 614-627.
[28] Chen P.J., Gurtin M.E., Williams W.O., 1968, A note on non-simple heat conduction, *Zeitschrift für Angewandte Mathematik und Physik* **19**: 969-970.
[29] Chen P.J., Gurtin M.E., Williams W.O., 1969, On the thermodynamics of non-simple elastic material with two temperatures, *Zeitschrift fur angewandte Mathematik und Physik* **20**: 107-112.
[30] Youssef H.M., 2006, Theory of two-temperature generalized thermoelasticity, *IMA Journal of Applied Mathematics* **71**: 383-390.
[31] Youssef H.M., Bassiouny E., 2008, Two-temperature generalized thermopiezoelasticity for one dimensional problems—State space approach, *Computational Methods in Science and Technology* **14**: 55-64.
[32] Islam M., Kanoria M., 2014, One-dimensional problem of a fractional order two-temperature generalized thermo-piezoelasticity, *Mathematics and Mechanics of Solids* **19**: 672-693.
[33] Kaur I., Lata P., 2019, Effect of hall current on propagation of plane wave in transversely isotropic thermoelastic medium with two temperature and fractional order heat transfer, *SN Applied Sciences* **1**: 900.
[34] Lata P., Kaur I., 2019, Thermomechanical interactions in transversely isotropic magneto thermoelastic solid with two temperatures and without energy dissipation, *Steel & Composite Structures* **32**: 779-793.
[35] Nowacki W., 1974, Dynamical problems of thermodiffusion in solids-I, *Bulletin of the Polish Academy of Sciences, Technical Sciences* **22**: 55-64.
[36] Nowacki W., 1974, Dynamical problems of thermodiffusion in solids-II, *Bulletin of the Polish Academy of Sciences, Technical Sciences* **22**: 129-135.
[37] Nowacki W., 1974, Dynamical problems of thermodiffusion in solids-III, *Bulletin of the Polish Academy of Sciences*, *Technical Sciences* **22**: 257-266.
[38] Sherief H.H., Hamza F.A., Saleh H.A., 2004, The theory of generalized thermoelastic diffusion, *International Journal of Engineering Science* **42**: 591-608.
[39] Kuang Z.B., 2010, Variational principles for generalized thermodiffusion theory in pyroelectricity, *Acta Mechanica* **214**: 275-289.
[40] Kumar R., Chawla V., 2012, General steady-state solution and Green's function in orthotropic piezothermoelastic diffusion medium, *Archives of Mechanics* **64**: 555-579.
[41] Kumar R., Sharma P., 2016, Analysis of plane waves in anisotropic piezothermoelastic diffusive medium, *Multidiscipline Modeling in Materials and Structures* **12**: 93-109.
[42] Kaur I., Lata P., 2019, Rayleigh wave popagation in transversely isotropic magneto thermoelastic medium with three-phase=lag heat transfer and diffusion, *International Journal of Mechanical and Materials Engineering* **14**: 12.
[43] Kansal T., 2019, Fundamental solution in the theory of thermoelastic diffusion materials with double porosity, *Journal of Solid Mechanics* **11**: 281-296.
[44] Bijarnia R., Singh B., 2004, Propagation of plane waves in an isotropic two-temperature thermoelastic solid half-space with diffusion, *Annals of Solid and Structural Mechanics* **6**: 37-45.